Hadronic Gas Models in Particle Production and Phase Transitions

Götz Mathias Weber

A thesis submitted in partial fulfilment of the
requirements for the degree of
Master Of Science
in the Department of Physics
University of Cape Town

March 1992

Contents

List of Figures

Chapter 1

The Canonical Description of Conserved Quantities

1.1 Introduction

In this work the methods of exact quantum number conservation in statistical mechanics are discussed and applied to the field of high energy nucleus-nucleus collisions. Various types of hadronic gas models are discussed as well as their merits and restrictions. Attempts to construct a phenomenological equation of state for nuclear matter are discussed in the context of the phase transition from hadronic matter to the quark-gluon plasma (QGP).

The fundamental difference between the nonrelativistic and relativistic scenaria is that whereas in the nonrelativistic limit particle numbers are conserved since the energies compared to the masses of the particles are small, in the relativistic case particles can be created from kinetic energy. Thus, in the relativistic scenario the conserved quantity is the conserved charge (e.g. baryon number, electric charge or strangeness which is usually dealt with by introducing a chemical potential), and not the particle numbers themselves which can take on all possible combinations provided that the charge Q remains fixed. It is clear that all conservation laws can be treated grand canonically by the introduction of a chemical potential for each conserved charge but in view of the number fluctuations inherent in this formalism it seems neccessary to employ the canonical formalism -which conserves the charge exactly- and to compare the results.

In the following section the partition function for a free, pointlike gas subject to the constraints of conserved baryon number B and strangeness S will be discussed. This is

of interest because these quantum numbers are conserved by the strong interaction which dictates the physics of high energy heavy ion collisions.

1.2 Exact Baryon and Strangeness Conservation

The way of incorporating quantum number conservation in statistical mechanics is to restrict the statistical trace to only those states having the required quantum number(s). This may be done by defining the Restricted Partition Function

$$Z_Q(T,V) = \frac{1}{2\pi}\int_0^{2\pi} d\phi \, \exp(-iQ\phi)\overline{Z}(T,V,\phi)$$

where Q refers to the (fixed) overall charge the gas possesses and $\overline{Z}(T,V,\phi)$ is the function obtained by substituting $\phi = -i\beta\mu$ in the usual statistical trace. Here μ is the chemical potential conjugate to the conserved charge(s). A derivation of this result may be found in [1],[2]. The extension to non-Abelian symmetries is possible, see [1], [3].

The starting point of the analysis is the partition function as presented by Hagedorn and Redlich [4]. The partition function differs from the one above in that now two quantum numbers Q_1, Q_2 are conserved so two angles ϕ and ψ are required:

$$Z_{Q_1,Q_2}(T,V) = \frac{1}{2\pi}\int_0^{2\pi} d\phi \, \exp(-iQ_1\phi)\frac{1}{2\pi}\int_0^{2\pi} d\psi \, \exp(-iQ_2\psi)\overline{Z}(T,V,\phi,\psi)$$

An extension of this work may be found in [5]. The methods of exact quantum number conservation for the cases where the gas is composed of particles having baryon number plus/minus one and strangeness plus/minus one, two or three will be investigated in the following sections. These quantum numbers correspond to the charges Q_1 and Q_2 above. A shorter version of the mathematical results presented here may be found in [6].

1.2.1 Case 1: Baryonnumber=±1, Strangeness=±1

Starting with the basic integral as presented by Hagedorn and Redlich with the angle ψ labelling the baryons and ϕ labelling the strange particles and assuming Boltzmann statistics one has for the canonical partition function $Z^1_{B,S}(T,V)$ (where the subscripts imply that one conserves B and S exactly and the superscript refers to the case where only particles with |strangeness| = 1 are included):

$$\begin{aligned} Z^1_{B,S}(T,V) &= Z_0 \frac{1}{2\pi}\int_0^{2\pi} d\phi \exp(-iS\phi)\frac{1}{2\pi}\int_0^{2\pi} d\psi \exp(-iB\psi) \\ &\cdot \exp\left(Z_K(\exp(i\phi)+\exp(-i\phi))\right) \\ &\cdot \exp\left(Z_N(\exp(i\psi)+\exp(-i\psi))\right) \\ &\cdot \exp\left(Z_Y(\exp(i(\psi-\phi))+\exp(-i(\psi-\phi)))\right) \end{aligned} \tag{1.1}$$

Here $Z_i(T,V)$ is the sum of all the one particle partition functions evaluated in the continuum limit corresponding to those particles having the same quantum numbers e.g.

$$Z_K \equiv Z_K + Z_{K^*} + ...$$

$$Z_N \equiv Z_N + Z_\Delta + ...$$

$$Z_Y \equiv Z_\Lambda + Z_{\Lambda^*} + ...$$

Explicitly, the one particle partition function for a given species of mass m_i and degeneracy g_i in a volume V at temperature T is given by:

$$\begin{aligned} Z_i(T,V) &= g_i V \int_{-\infty}^{\infty} \frac{d^3p}{(2\pi)^3}\exp(-\epsilon_i/T) \\ &= \frac{g_i}{2\pi^2} V m^2 T K_2(\frac{m_i}{T}) \end{aligned}$$

where $K_2(x)$ is the modified Bessel function of order 2. Thus one has for the partition function

$$\begin{aligned} Z^1_{B,S}(T,V) &= Z_0 \frac{1}{2\pi}\int_0^{2\pi} d\phi \exp(-iS\phi)\frac{1}{2\pi}\int_0^{2\pi} d\psi \exp(-iB\psi) \\ &\cdot \exp\left(2Z_K\cos(\phi)+2Z_N\cos(\psi)+2Z_Y\cos(\phi-\psi)\right) \end{aligned} \tag{1.2}$$

Z_0 is the multiplicative part originating from those particles not possessing either of the quantum numbers e.g. the pions. The introduction of a "1" in the form of a Delta function allows the decoupling of the angles ϕ and ψ which would otherwise prevent the integral from

being solved analyically for the case where the strangeness is plus/minus two or three.
We make use of the following (Fourier) representation of the Delta function:

$$\delta(x) = \frac{1}{2\pi} \sum_{n=-\infty}^{\infty} \exp(inx)$$

Choosing the variable x to be $\phi - \psi - \alpha$ one obtains

$$\begin{aligned} Z^1_{B,S}(T,V) &= Z_0 \frac{1}{2\pi} \int_0^{2\pi} d\phi \exp(-iS\phi) \frac{1}{2\pi} \int_0^{2\pi} d\psi \exp(-iB\psi) \\ &\cdot \exp(2Z_K \cos(\phi) + 2Z_N \cos(\psi) + 2Z_Y \cos(\phi - \psi)) \\ &\cdot \sum_{n=-\infty}^{\infty} \frac{1}{2\pi} \int_0^{2\pi} d\alpha \exp(in(\phi - \psi - \alpha)) \end{aligned} \tag{1.3}$$

Making use of the delta function one may now decouple the angles for the hyperon particles as

$$\begin{aligned} \exp(2Z_Y \cos(\phi - \psi)) &= \sum_{n=-\infty}^{\infty} \frac{1}{2\pi} \int_0^{2\pi} d\alpha \exp(in(\phi - \psi - \alpha)) \exp(2Z_Y \cos(\alpha)) \\ &= \sum_{n=-\infty}^{\infty} \exp(in(\phi - \psi)) I_n(2Z_Y) \end{aligned} \tag{1.4}$$

where use has been made of the integral representation of the Bessel function of order B:

$$I_B(x) = \frac{1}{2\pi} \int_0^{2\pi} d\theta \exp(x \cos(\theta)) \exp(-iB\theta) .$$

Thus one has for the partition function

$$\begin{aligned} Z^1_{B,S}(T,V) &= Z_0 \sum_{n=-\infty}^{\infty} \frac{1}{2\pi} \int_0^{2\pi} d\phi \exp(-iS\phi + in\phi) \\ &\cdot \frac{1}{2\pi} \int_0^{2\pi} d\psi \exp(-iB\psi - in\psi) \\ &\cdot \exp(2Z_K \cos(\phi)) \exp(2Z_N \cos(\psi)) \end{aligned} \tag{1.5}$$

and performing the integrations one is left with the result

$$Z^1_{B,S}(T,V) = Z_0 \sum_{n=-\infty}^{\infty} I_n(2Z_Y) I_{S-n}(2Z_K) I_{B+n}(2Z_N) \tag{1.6}$$

It is important to realize that the overall strangeness of the gas has the arbitrarily large value S and is composed (in this case) of particles having |strangeness| = 1 i.e. the kaons and the hyperons.

The canonical partition function for a gas with two conserved charges has been evaluated. The question now is how to obtain the particle numbers; in the usual canonical formalism where charge is not conserved the particle number is fixed by construction, here the overall charge of the gas has been fixed so how does one obtain these numbers? They can be obtained by introducing an additional chemical potential for each particle sort and then making use of the standard grand canonical method to project them out:

$$\mathrm{N}_i = \frac{T}{Z}\left(\frac{\partial Z}{\partial \mu_i}\right)\Big|_{\mu_i=0} \tag{1.7}$$

here N_i is the particle number conjugate to the chemical potential μ_i i.e. one treats each particle sort as if it were a conserved quantity. Notice that all the chemical potentials have been set to zero after differentiation: this has to be done so that one remains within the canonical formalism. Thus one has the rule that with respect to particle numbers one has to use the grand canonical description while for the conservation law one has the choice between the grand canonical and the canonical formalism [4].
Using the above prescription the particle numbers follow as:

$$\begin{aligned}
\langle N_{\frac{K}{\bar{K}}}\rangle &= Z_0 \frac{Z_K(T,V)}{Z} \sum_{n=-\infty}^{\infty} I_n(2Z_Y) I_{n+B}(2Z_N) I_{S-n\mp 1}(2Z_K) \\
\langle N_{\frac{N}{\bar{N}}}\rangle &= Z_0 \frac{Z_N(T,V)}{Z} \sum_{n=-\infty}^{\infty} I_n(2Z_Y) I_{n+B\mp 1}(2Z_N) I_{S-n}(2Z_K) \\
\langle N_{\frac{Y}{\bar{Y}}}\rangle &= Z_0 \frac{Z_Y(T,V)}{Z} \sum_{n=-\infty}^{\infty} I_{n\pm 1}(2Z_Y) I_{n+B}(2Z_N) I_{S-n}(2Z_K)
\end{aligned} \tag{1.8}$$

The results presented above may be found in [7]. They were used to predict strange particle abundances in small volumes of hot hadronic gases in $\overline{p}$-nucleus annihilations.

1.2.2 Case 2: Baryonnumber=±1, Strangeness=±2

In this case one includes the Ξ and $\overline{\Xi}$ which have strangeness $\mp$ 2 respectively: the Z_Ξ term in the partition function now contains the angle 2ϕ. The partition function in its integral form reads:

$$\begin{aligned}
Z^2_{B,S}(T,V) \;=\; & Z_0 \frac{1}{2\pi}\int_0^{2\pi} d\phi \exp\left(-iS\phi\right) \frac{1}{2\pi}\int_0^{2\pi} d\psi \exp\left(-iB\psi\right) \\
& \cdot \exp\left(2Z_K \cos\left(\phi\right) + 2Z_N \cos\left(\psi\right)\right) \\
& \cdot \exp\left(2Z_Y \cos\left(\phi-\psi\right) + 2Z_\Xi \cos\left(\psi-2\phi\right)\right)
\end{aligned} \tag{1.9}$$

Before decoupling the angles ϕ and ψ it is useful to separate the angles of the Z_Ξ term into exponentials which enables one to use an alternative generating function of the Bessel polynomials :

$$\exp\left(\frac{x}{2}(t+\frac{1}{t})\right) = \sum_{m=-\infty}^{\infty} t^m I_m(x)$$

Setting $x = 2Z_\Xi$ and $\exp(i(\psi - 2\phi)) = t$ the result for the partition function follows

$$\begin{aligned} \mathrm{Z}^2_{B,S}(T,V) &= Z_0 \frac{1}{2\pi}\int_0^{2\pi} d\phi \exp(-iS\phi)\frac{1}{2\pi}\int_0^{2\pi} d\psi \exp(-iB\psi) \\ &\cdot \exp(2Z_K\cos(\phi) + 2Z_N\cos(\psi) + 2Z_Y\cos(\phi-\psi)) \\ &\cdot \sum_{m=-\infty}^{\infty} I_m(2Z_\Xi)\exp(im(\psi-2\phi)) \end{aligned} \tag{1.10}$$

Introducing the Delta function to decouple ϕ and ψ again one obtains

$$\begin{aligned} \mathrm{Z}^2_{B,S}(T,V) &= Z_0 \sum_{m=-\infty}^{\infty} I_m(2Z_\Xi) \\ &\cdot \sum_{n=-\infty}^{\infty}\frac{1}{2\pi}\int_0^{2\pi} d\phi \exp(-i(S-n+2m)\phi)\exp(2Z_K\cos(\phi)) \\ &\cdot \frac{1}{2\pi}\int_0^{2\pi} d\psi \exp(-i(B+n-m)\psi)\exp(2Z_N\cos(\psi)) \\ &\cdot \frac{1}{2\pi}\int_0^{2\pi} d\alpha \exp(-in\alpha)\exp(2Z_Y\cos(\alpha)) \end{aligned} \tag{1.11}$$

and thus the partition function reads in closed form:

$$\begin{aligned} \mathrm{Z}^2_{B,S}(T,V) &= Z_0 \sum_{m=-\infty}^{\infty} I_m(2Z_\Xi) \\ &\cdot \sum_{n=-\infty}^{\infty} I_{S-n+2m}(2Z_K) I_{B+n-m}(2Z_N) I_n(2Z_Y) \end{aligned} \tag{1.12}$$

The particle numbers follow as

$$\begin{aligned} \langle N_{\frac{K}{\bar{K}}}\rangle &= Z_0 \frac{Z_K(T,V)}{Z}\sum_{m=-\infty}^{\infty} I_m(2Z_\Xi)\sum_{n=-\infty}^{\infty} I_{n\pm1-S-2m}(2Z_K) \\ &\cdot I_{n+B-m}(2Z_N) I_n(2Z_Y) \end{aligned}$$

$$\begin{aligned} \langle N_{\frac{N}{\bar{N}}}\rangle &= Z_0 \frac{Z_N(T,V)}{Z}\sum_{m=-\infty}^{\infty} I_m(2Z_\Xi)\sum_{n=-\infty}^{\infty} I_{n-2m-S}(2Z_K) \\ &\cdot I_{n+B-m\mp1}(2Z_N) I_n(2Z_Y) \end{aligned}$$

$$\begin{aligned} \langle N_{\frac{Y}{\bar{Y}}}\rangle &= Z_0 \frac{Z_Y(T,V)}{Z}\sum_{m=-\infty}^{\infty} I_m(2Z_\Xi)\sum_{n=-\infty}^{\infty} I_{n-2m-S}(2Z_K) \\ &\cdot I_{n+B-m}(2Z_N) I_{n\pm1}(2Z_Y) \end{aligned}$$

$$\langle N_{\overset{\Xi}{\overline{\Xi}}} \rangle = Z_0 \frac{Z_\Xi(T,V)}{Z} \sum_{m=-\infty}^{\infty} I_m(2Z_\Xi) \sum_{n=-\infty}^{\infty} I_{n-2m-S\mp 2}(2Z_K) \cdot I_{n+B-m\mp 1}(2Z_N) I_n(2Z_Y) \tag{1.13}$$

One sees that two infinite sums appear: one from the Delta function and the other from the generating function of the Bessel polynomials.

1.2.3 Case 3: Baryonnumber=±1, Strangeness=±3

This is the most complete case since now all the particles of the hadronic spectrum may be included in the gas.

From first principles one has for the partition function in its integral form:

$$\begin{aligned} Z^3_{B,S}(T,V) = Z_0 \frac{1}{2\pi} \int_0^{2\pi} d\phi \exp(-iS\phi) \frac{1}{2\pi} \int_0^{2\pi} d\psi \exp(-iB\psi) \\ \cdot \sum_{n=-\infty}^{\infty} \frac{1}{2\pi} \int_0^{2\pi} d\alpha \exp(in(\phi - \psi - \alpha)) \\ \cdot \exp(2Z_K \cos(\phi)) \exp(2Z_N \cos(\psi)) \exp(2Z_Y \cos(\phi - \psi)) \\ \cdot \exp(2Z_\Xi \cos(2\phi - \psi) + 2Z_\Omega \cos(3\phi - \psi)) \end{aligned} \tag{1.14}$$

Performing the integrations one obtains for the partition function

$$\begin{aligned} Z^3_{B,S}(T,V) = Z_0 \sum_{k=-\infty}^{\infty} I_k(2Z_\Xi) \sum_{m=-\infty}^{\infty} I_m(2Z_\Omega) \\ \cdot \sum_{n=-\infty}^{\infty} I_n(2Z_Y) I_{S-n-2k-3m}(2Z_K) I_{B+n+k+m}(2Z_N) \end{aligned} \tag{1.15}$$

The particle numbers follow as

$$\begin{aligned} \langle N_{\overset{K}{\overline{K}}} \rangle = Z_0 \frac{Z_K(T,V)}{Z} \sum_{k=-\infty}^{\infty} I_k(2Z_\Xi) \sum_{n=-\infty}^{\infty} I_n(2Z_Y) \\ \cdot \sum_{m=-\infty}^{\infty} I_{S\pm 1-n-2k-3m}(2Z_K) I_{B+n+k+m}(2Z_N) I_m(2Z_\Omega) \end{aligned}$$

$$\begin{aligned} \langle N_{\overset{N}{\overline{N}}} \rangle = Z_0 \frac{Z_N(T,V)}{Z} \sum_{k=-\infty}^{\infty} I_k(2Z_\Xi) \sum_{n=-\infty}^{\infty} I_n(2Z_Y) \\ \cdot \sum_{m=-\infty}^{\infty} I_{S-n-2k-3m}(2Z_K) I_{B+n+k+m\mp 1}(2Z_N) I_m(2Z_\Omega) \end{aligned}$$

$$\begin{aligned} \langle N_{\overset{Y}{\overline{Y}}} \rangle = Z_0 \frac{Z_Y(T,V)}{Z} \sum_{k=-\infty}^{\infty} I_k(2Z_\Xi) \sum_{n=-\infty}^{\infty} I_{n\pm 1}(2Z_Y) \\ \cdot \sum_{m=-\infty}^{\infty} I_{S-n-2k-3m\pm 1}(2Z_K) I_{B+n+k+m\mp 1}(2Z_N) I_m(2Z_\Omega) \end{aligned}$$

$$\langle N_{\substack{\Xi \\ \Xi}} \rangle = Z_0 \frac{Z_\Xi(T,V)}{Z} \sum_{k=-\infty}^{\infty} I_k(2Z_\Xi) \sum_{n=-\infty}^{\infty} I_{n\pm1}(2Z_Y) \cdot \sum_{m=-\infty}^{\infty} I_{S-n-2k-3m\pm2}(2Z_K) I_{B+n+k+m\mp1}(2Z_N) I_m(2Z_\Omega)$$

$$\langle N_{\substack{\Omega \\ \Omega}} \rangle = Z_0 \frac{Z_\Omega(T,V)}{Z} \sum_{k=-\infty}^{\infty} I_k(2Z_\Xi) \sum_{n=-\infty}^{\infty} I_{n\pm1}(2Z_Y) \cdot \sum_{m=-\infty}^{\infty} I_{S-n-2k-3m\pm3}(2Z_K) I_{B+n+k+m\mp1}(2Z_N) I_m(2Z_\Omega) \qquad (1.16)$$

One infinite summation comes from the Delta function whereas the other two come from decoupling the multiple angles 2ϕ and 3ϕ respectively.

This section concludes the derivation of the particle numbers in the exact baryon number and strangeness formalism. The results will be used in the section "Hadron Gas Models" where particle numbers will be predicted which originate from the thermalised gas produced in the collision of nuclei.

1.3 Convergence Properties

The canonical partition functions for a gas with two conserved charges have been derived. One may choose one of three partition functions: $Z^1_{B,S}(T,V)$ is the one to use if one wishes to consider a gas where the strangeness is carried only by the kaons, $Z^2_{B,S}(T,V)$ is the one if one includes Ξ (and kaons) and $Z^3_{B,S}(T,V)$ is the one to use if one includes the Ω (and Ξ and kaons). The equations for the respective particle numbers involve at least one infinite summation over indexed Bessel functions. The question is how useful are these expressions; can they be evaluated numerically?

In the following figures the magnitude of $Z^1_{B,S}(T,V)/Z_0$ is plotted against the running index n. The gas was composed of 56 particles including antiparticles. Clearly the convergence of the series is very rapid and the summation is centred about the index $n = 0$; see Figure 1.1. Figure 1.2 shows a similar plot, this time for a gas having baryonnumber 5 at the same temperature and volume. The magnitude of the partition function decreases markedly and the summation becomes centred around small values of negative n. Figure 1.3 is the result of a calculation performed in a larger volume thus increasing the arguments of the Bessel functions. Although the magnitude of the partition function increases dramatically, convergence

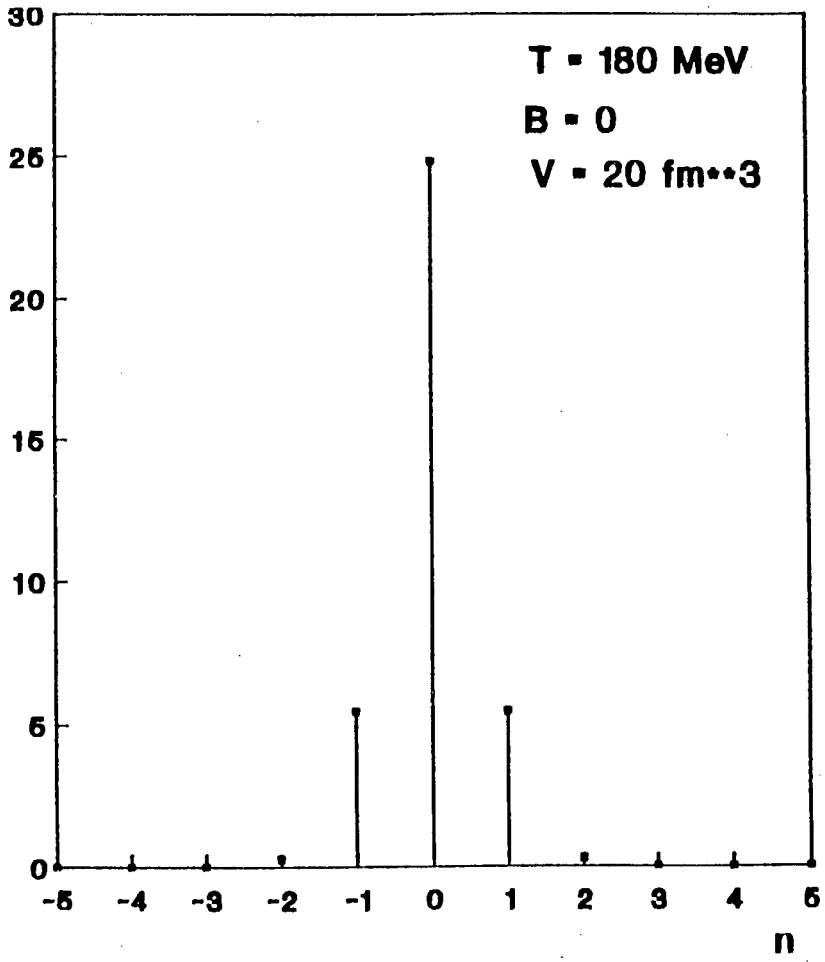

Figure 1.1: Magnitude of $Z^1_{B,S}(T,V)/Z_0$ as a function of index n for a baryonless and zero strangeness gas at $T = 180$ MeV and $V = 20$ fm^3. Taken from [6].

is still very rapid.

Further investigation showed that the largest terms in the sum were centred about the negative value of B chosen. Only a few iterations of the index n were neccessary to obtain accurate results: for a given value of B it was sufficient to sum from $B - 10$ to $B + 10$. For the $Z^3_{B,S}(T,V)$ particle numbers this already meant at least 8000 sums of Bessel functions; the computer time increased dramatically when calculating particle numbers derived from $Z^3_{B,S}(T,V)$ compared to $Z^2_{B,S}(T,V)$. The differences in particle numbers these equations predicted will be demonstrated in the next chapter.

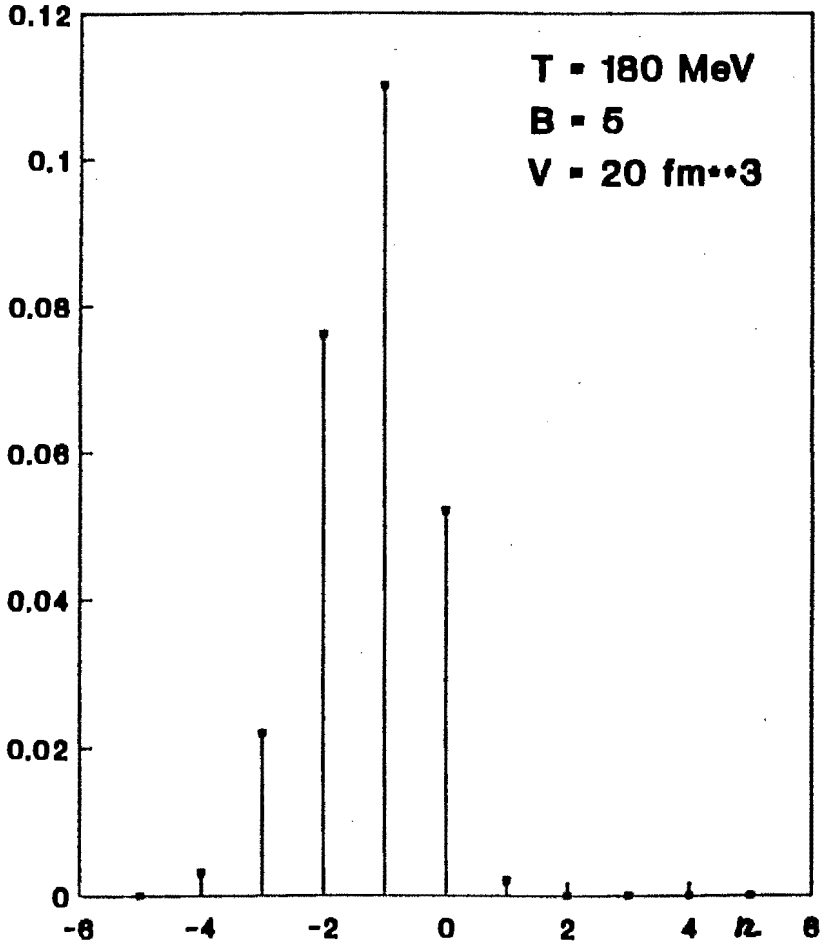

Figure 1.2: Magnitude of $Z^1_{B,S}(T,V)/Z_0$ as a function of index n for a gas with baryonnumber 5 and zero strangeness at $T = 180$ MeV and $V = 20$ fm^3. Taken from [6].

1.4 Finite Volume Effects

A direct consequence of imposing exact quantum number conservation is that particle numbers are not additive i.e. the usual relationship that

$$N(V_1) + N(V_2) = N(V_1 + V_2)$$

is not fulfilled for finite volumes. This can easily be seen from equation (1.8): consider the number of kaons in two volumes V_1 and V_2.

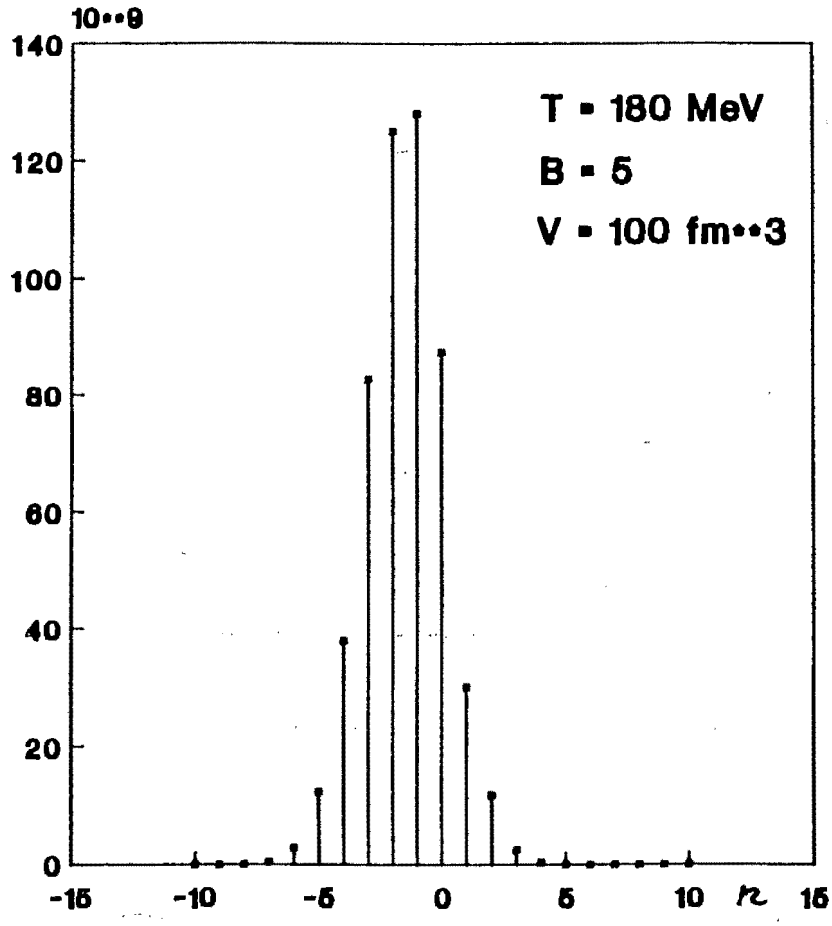

Figure 1.3: Magnitude of $Z^1_{B,S}(T,V)/Z_0$ as a function of index n for a gas with baryonnumber 5 and zero strangeness at $T = 180$ MeV and $V = 100$ fm^3. (Note magnitude of ordinate). Taken from [6].

One has

$$\begin{aligned}\langle N_K(V_1)\rangle + \langle N_K(V_2)\rangle &= Z_0 \frac{Z_K(T,V_1)}{Z} \sum_{n=-\infty}^{\infty} I_n(2Z_Y(V_1)) I_{n+B}(2Z_N(V_1)) I_{S-n-1}(2Z_K(V_1)) \\ &\quad + Z_0 \frac{Z_K(T,V_2)}{Z} \sum_{n=-\infty}^{\infty} I_n(2Z_Y(V_2)) I_{n+B}(2Z_N(V_2)) I_{S-n-1}(2Z_K(V_2)) \\ &\neq Z_0 \frac{Z_K(T,(V_1+V_2))}{Z} \\ &\quad \cdot \sum_{n=-\infty}^{\infty} I_n(2Z_Y(V_1+V_2)) I_{n+B}(2Z_N(V_1+V_2)) I_{S-n-1}(2Z_K(V_1+V_2))\end{aligned} \tag{1.17}$$

The one particle partition function $Z_K(T,V)$ is linear in the volume and in the usual canonical formalism this allows particle number additivity but in the case above the infinite summations prevent this; the sums can be understood as "correction factors" to the usual canonical

particle numbers.

Indeed, the correspondence between the exact B and S partition function $Z_{B,S}(T,V)$ and the grand canonical one has been established to be exact by Hagedorn and Redlich [4] in the limit of large B and S.

1.5 Conclusion

The partition function for a gas with two conserved quantum numbers has been presented in closed form, albeit as infinite sums over Bessel functions. Numerically, these sums turn out to converge rapidly -even for large volumes.

This section then concludes the derivation of the particle numbers in the exact B and S formalism; the results will be used in the following chapter where particle ratios will be predicted which originate from the thermalised gas produced in the collisions of nuclei.

Chapter 2

Modelling Particle Production In Ion Collisions

2.1 Hadron Gas Models

Experiments performed at accelerators yield, amongst other things, information about particle numbers produced at chosen projectile energies and target. The question arises whether one can model these observed numbers in an equilibrium statistical picture: does it make sense to attempt to model a process occuring in a very small volume (of the order of multiple nuclear volumes) and over very short periods of time? The predictions of statistical mechanics after all are expected to apply firstly in the infinite volume limit and secondly ensemble theory presupposes the validity of the ergodic theorem [1]. This then raises the interesting question whether processes occuring in very short periods of time sufficiently populate all the microstates of the ensemble so that statistical physics applies to the macrostate or whether certain subsystems are populated preferentially and a bias towards these states is observed in the result. Simulating nuclear collisions with nonequilibrium thermodynamics is a formidable task: one has to know the cross-section for each possible process in order to construct the rate equation. In this work only equilibrium techniques will be assumed.
Statistical modelling of particle production has a twofold aim: can the observed particle numbers be accomodated in a thermodynamical picture (of a free relativistic gas, or at least nearly free) and if so, what can one learn about the process i.e. what is the temperature of the gas and what is its baryon density and furthermore, should the predictive power of the model fail only for strange particles, does this indicate the formation of the quark gluon

[1] This states that the time average of an observable may be replaced with its ensemble average.

plasma in energetic collisions [8],[9] ?

The experimental support for the thermodynamic picture comes from the measured particle spectra from which one can then dedeuce the temperature [10]. Plotting $m_t^{\frac{-3}{2}} dn/dm_t$ vs m_t (with m_t being the transverse mass normalised to m_t = m for all particles) shows the exponentially decreasing trend as predicted by the differential Boltzmann density. This is the proof that thermal models provide a good first approximation to the particle production rates as observed in collisions and that a common temperature may be used to describe all the species in the gas. Information about the volume of the fireball system can be obtained from interferometric methods. The baryon chemical potential used in grand canonical models can be obtained from the $\frac{\overline{\Lambda}}{\Lambda}$ ratio. The overall zero strangeness of the gas fixes the strange chemical potential. Thus, in principle, all the parameters needed to employ free gas models are available from experiment. Interacting gas models require more parameters (strengths of interactions etc.) but these are also experimentally known, albeit often only for normal nuclear matter. In this work all parameters required are fitted to reproduce the observed particle ratios and none have been extracted directly from experiment.

2.2 Hadron Gas Models in Action

The motivation for hadronic gas models has been presented in the previous section. At this stage we wish to investigate how successful they are. There are then three formalisms in statistical physics at one's disposal with which to model the processes where baryon number and strangeness are conserved:

- grand canonical. Variables are μ_B, μ_S, T as used in [11]
- mixed canonical. Variables are μ_B, S, T as used in [12]
- canonical. Variables are B, S, T, V

where μ_B is the baryon chemical potential and μ_S is the strange chemical potential. S is the strangeness of the gas, B the baryon number, V the volume and T the temperature. We will investigate the canonical formalism where baryon number and strangeness are conserved exactly and compare it to the grand canonical approach which is generally used to predict particle ratios or multiplicities. At this point it is worthwhile to stress that the grand canonical

formalism explicitly deals with conserved quantities of a given species. This can be seen directly from the thermodynamical trace

$$Z = \mathrm{Tr}\, e^{\frac{-(E-\mu N)}{T}}$$

where the chemical potential governs only the conserved quantities and not the particle numbers as a whole. Thus, in the framework of the thermal models, pions, which are not assigned a chemical potential because they do not carry either strangeness or baryon number are produced proportional to the temperature.

The assumption made when using these models is that relative chemical equilibrium exists. This means that chemical reactions are taking place at the same rate both in the forward and reverse direction. This is the basic assumption of equilibrium statistical mechanics. Thermalisation means that the particles produced in the fireball have interacted sufficiently so that a common temperature may be used to describe all species in the gas. Thus thermal equilibrium means that the particles' momenta are distributed according to the equilibrium statistical mechanics and chemical equilibrium means that the abundances are dictated by the particles' statistical weight. The question whether thermalisation indeed occurs has recently been addressed by Davidson et al. [13] who found that an equilibrium statistical model with hadronic interactions incorporated in a mean field way reproduced the WA 85 and NA 35 data; only the pion multiplicities remained a problem: the models predicted less than observed. The problem of the pion multiplicities will be addressed in the next section. Finite size effects incorporated by modifying the phase space volume element to include surface and linear terms in the momentum distribution were found to be small because the volumes were of the order of 500 fm^3. That the system becomes thermalised seems to be a weaker requirement than chemical equilibration; the time scales for the two processes are very different. It seems plausible that thermal equilibrium is attained far more rapidly than chemical equilibrium; for thermal equilibrium one requires an interaction between particles of any type whereas for chemical equilibration certain reactions are required for which there may not be enough time so that full equilibration is attained. However, the successes of these models in predicting observables gives one faith in the statistical picture provided that it includes the basic physical requirements: baryons are extended objects and volume corrections play an important role in fixing e.g. the baryon density; it is unrealistic to use point-like particle expressions when dealing with extended objects. For temperatures of the

order of hundreds of MeV's resonance production and decay into pions and kaons must be included as a basic ingredient. It is important to note that because hadronic gas models presuppose equilibration - both chemical and thermal - all information about the early history of the fireball is lost. The predictive power of these models is restricted to the very last instance of the fireball's existence; the freeze-out. Experimental data very different from model predictions could point to

- model deficiency: no equilibration
- violent reactions in the fireball (fragmentation, hot spots, jets)
- QGP production in early phase of fireball's existence

Information about the early history of the fireball is mediated by particles that do not interact with the secondaries and thus retain their 'memory' of the early period. The dileptons are such particles -they are essentially a clock for the hadron gas lifetime- but their spectrum (which is modified by the existence of the fireball) is experimentally ambiguous [14].
A strength of these models is that they allow calculation of densites other than the 4π value. This can de done by changing the spherically symmetrical momentum distribution $d^3p = 4\pi p^2 dp$ to a cylindrically symmetrical one corresponding to the experimental setup: $d^3p = 2\pi p_t dp_t dp_l$ (with $E = \sqrt{m^2 + p_t^2 + p_l^2}$) and infinite integration over the longitudinal component of the momentum (p_l) is understood. The lower bound on p_t can then be set to the experimental p_t cut. This is an advantage these models have: one can quite easily investigate the particle production in a specific dynamical window. Not only is the experimental data not the 4π value, it is also measured in a specific rapidity window. This has an important consequence: the temperature obtained from the m_t spectrum is thus only an effective temperature applying to the particles at midrapidity –at first sight. However, if one invokes the Bjorken picture [15] of particle collisions, the p_t spectrum of particles produced is independent of the rapidity y. It is clear that the under this assumption the experimental data measured in a specific window will differ from the y-integrated data by a constant factor. Given the overall success of the Bjorken model, let us see how these statistical formalisms perform when one attempts to reproduce the experimental data if one makes this assumption.

The experimental situation at present is as follows: at ISR energies (p-p collisions) at midrapidity the K/π ratios were approximately 11% [16]. The E 802 Collaboration at BNL

[17] have measured the K/π ratios in the central rapidity region of Si-Au and Si-Cu collisions (14.6 GeV per nucleon) to be:

$$\frac{K^+}{\pi^+} = 19.2 \pm 3\%$$
$$\frac{K^-}{\pi^-} = 3.6 \pm 0.8\%$$

and at CERN the WA 85 [18] and NA 35 [19] collaboration (S-W and S-S collisions respectively) measured the following strange baryon ratios :

$$\frac{\overline{\Lambda}}{\Lambda} = 19 \pm 1\%$$
$$\frac{\overline{\Xi}}{\Xi} = 36 \pm 7\%$$

The K^-/π and $\overline{\Lambda}/\Lambda$ ratios do not show significant increases when one goes from p-p to heavy ion collisions, however the K^+/π and $\overline{\Xi}/\Xi$ ratios do. The question is whether one can understand these increases as a volume increases in the statistical picture.

The K/π ratios can be reproduced using a hadron gas model with the parameters T=100 MeV and baryon density $n_B \sim 0.1/\text{fm}^3$ although the error bars on the data allow values of $0.02 \leq n_B \leq 0.17$, see [11]. The CERN data obtained at the higher projectile energy of 200 GeV per nucleon can be acommodated at a larger baryon density of $n_B \sim 0.12/\text{fm}^3$ and a higher temperature of approximately 180 to 200 MeV. Note that the higher temperature neccessarily implies a greater meson density as this grows proportional to T^3 in the massless limit. The models used to predict the particle ratios are typically grand canonical with respect to baryon chemical potential and strange chemical potential [11] or mixed canonical e.g. exact strangeness conservation and grand canonical with respect to baryon number [12] and [20]. This can be justified provided the baryon number of the gas is sufficiently large so that the particle number fluctuations inherent in the grand canonical formalism are not important. When investigating the particles produced in p-p collisions, it is not justifiable to use the grand canonical approach; this has been advocated by Hagedorn for some time [21]. The concept of an infinite heat bath of baryons and mesons is clearly not sensible when dealing with a gas of baryonnumber two.

The production of strange baryons in a small volume is not favoured since these are relatively massive particles ($\sim$ 1 GeV) and secondly they have to be accompanied by an antistrange baryon or meson making the total expenditure in energy not less than 2 GeV. As the interaction volume increases it becomes easier to produce these particles and one explains the

observed increase in antistrange baryons to strange baryons as one collides heavier nuclei this way. Kaons are light strange particles produced significantly in p-p collisions but even more so in heavy ion collisions; in excess of a factor of 1.5, even when the data is rescaled. This can be explained by assuming a greater interaction volume for the gas as well as noting that the strange chemical potential increases rapidly with increasing baryon chemical potential thus leading to a greater production in the number of K^+. Consequently, as the baryon content in the gas increases, the K^-/π^- and K^+/π^+ ratios diverge. Figures 2.1 and 2.2 are the K/π ratios obtained from a grand canonical hadron gas model with three hard-core radii and temperatures, taken from [11]. As can be seen, the grand canonical approach can

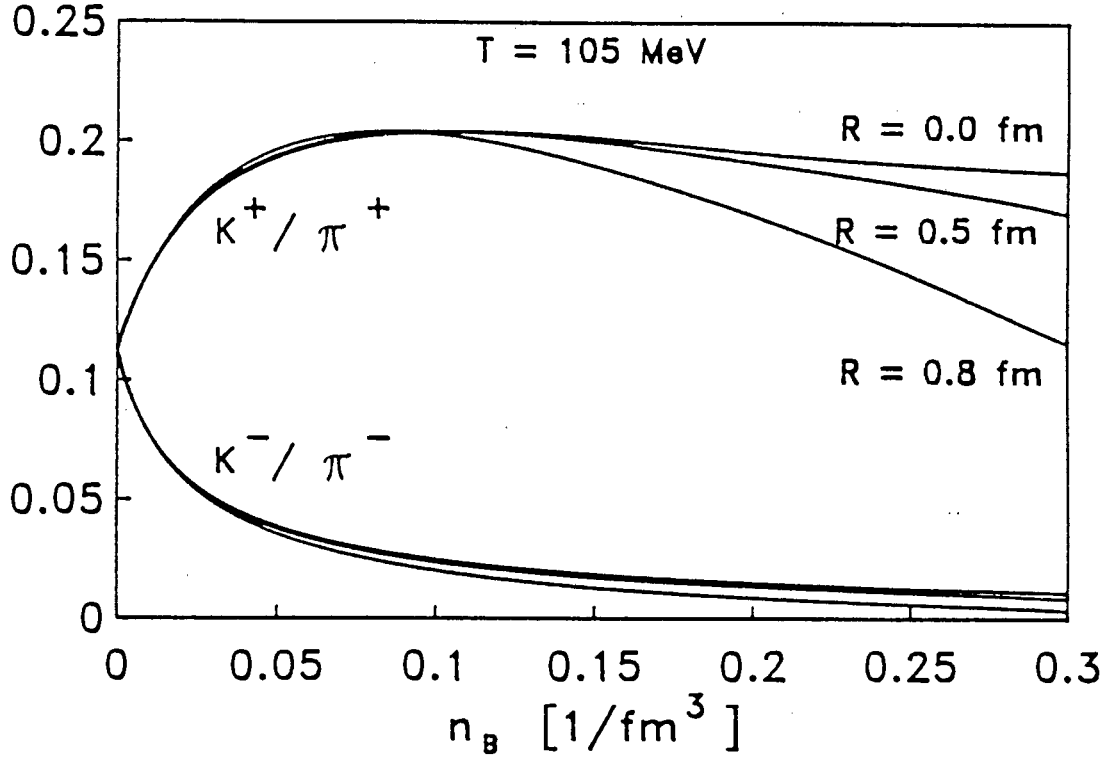

Figure 2.1: K/π ratios in grand canonical model as a function of baryon density n_B and hard core baryon radius R. Taken from [11].

be justified for heavy ion collisions; the data measured can be fitted quite well. Figure 2.3 shows the exactly conserved baryon and strangeness result with the variables temperature, volume and baryonnumber. The plot comes from [6] with the Si-Au data point corrected, in

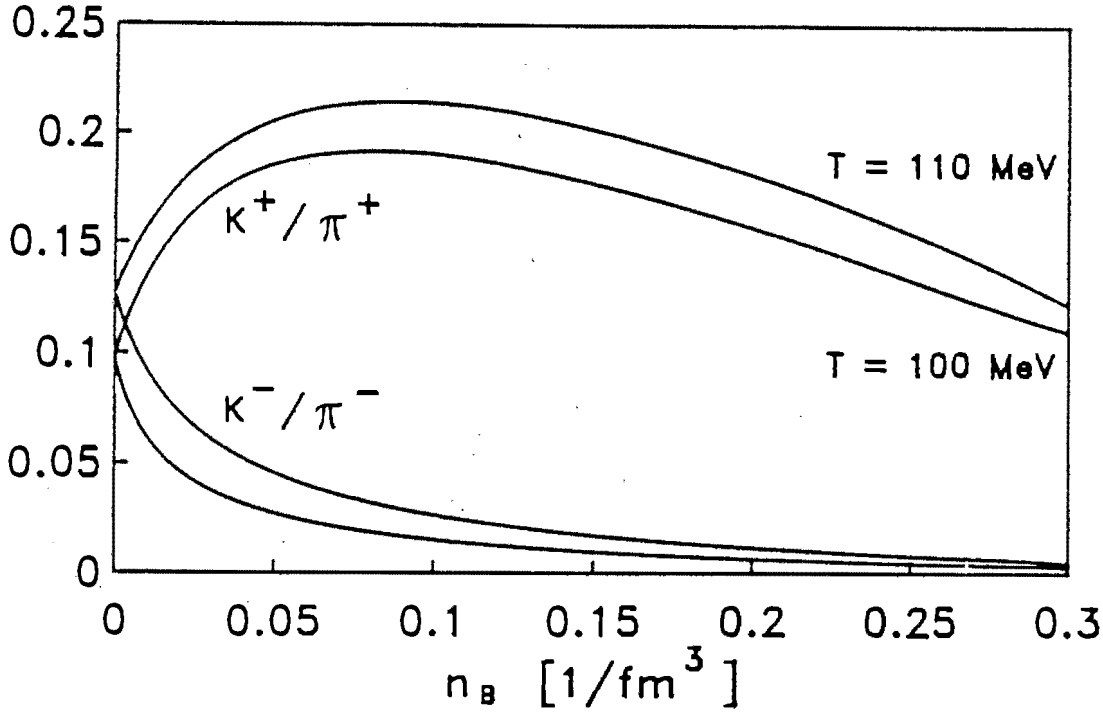

Figure 2.2: K/π ratios in grand canonical model as a function of baryon density for two temperatures T=100 MeV and T=110 MeV. Taken from [11].

the published paper the volume was calculated incorrectly.

The grand canonical formalism can clearly be justified in the case of Si-Au and Si-Cu collisions but small volume effects are manifest in the p-p, p-Cu results. To reproduce these results the mixed canonical or B , S exact formalism is neccessary. For a fixed baryon density $n_B = B/V$ but B , $V \to \infty$ one obtains the grand canonical results since particle fluctuations in the grand canonical ensemble behave as $\frac{1}{\sqrt{N}}$.

The freeze out volume for the reaction system is obtained by considering the following geometrical picture: a given projectile of radius R_P and mass number A_P bores a volume V_{in} out of the target given by :

$$V_{in} = \pi R_P^2 \, 2R_T = \frac{3}{2} V_0 A_P^{\frac{2}{3}} A_T^{\frac{1}{3}} \tag{2.1}$$

The target is labelled with the subscripts T and V_0 is the volume of a baryon. The baryon number B inside this volume is

$$B = A_P + \frac{V_{in}}{V_T} A_T \tag{2.2}$$

After the collision the system expands up to the freeze out time after which the hadrons cease to interact. This expansion is characterised by the parameter α. The pointlike baryon density n_B^0 is given by

$$n_B^0 = \frac{B}{\alpha V_{in}} \tag{2.3}$$

and the extended baryon density n_B is given by

$$n_B = \frac{B}{\alpha V_{in} + B V_0} \tag{2.4}$$

which follows from reducing the available pointlike volume by B times the volume of a baryon:

$$V_{\text{point-like}} = V - B V_0 \tag{2.5}$$

For a baryon density of $0.1/\text{fm}^3$ the expansion parameter and freeze out volume (given by $\alpha \cdot V_{in}$) can be determined:

1. Si-Au collisions: α =4.95, freeze out volume V_{Si-Au}= 398 V_0
2. p-Au collisions: α =4.1, freeze out volume V_{p-Au}= 36 V_0
3. p-Cu collisions: α =4.3, freeze out volume V_{p-Cu}= 26 V_0
4. p-p collisions: α =7.3, freeze out volume V_{p-p}= 7 V_0

For the p-p collisions we took $V_{in} = V_0$ with $B = 2$.

The results obtained for K^-/π^- and K^+/π^+ ratios using the particle numbers derived from the $Z^3_{B,S}(T,V)$ and $Z^2_{B,S}(T,V)$ equations is presented in Figure 2.4. The curves cannot be disentangled at at large volumes however at small volumes the production of an Ω has to be accompanied by at least three kaons, that is why the K^+/π^+ ratio increases more rapidly than in the strangeness=$\pm$2 case. One observes a slight decrease in the K^+/π^+ ratio, as calculated with 124 resonances (cut-off mass about 2 GeV) when compared to a hadronic gas containing 56 resonances (cut-off mass about 1.6 GeV). This can easily be explained by

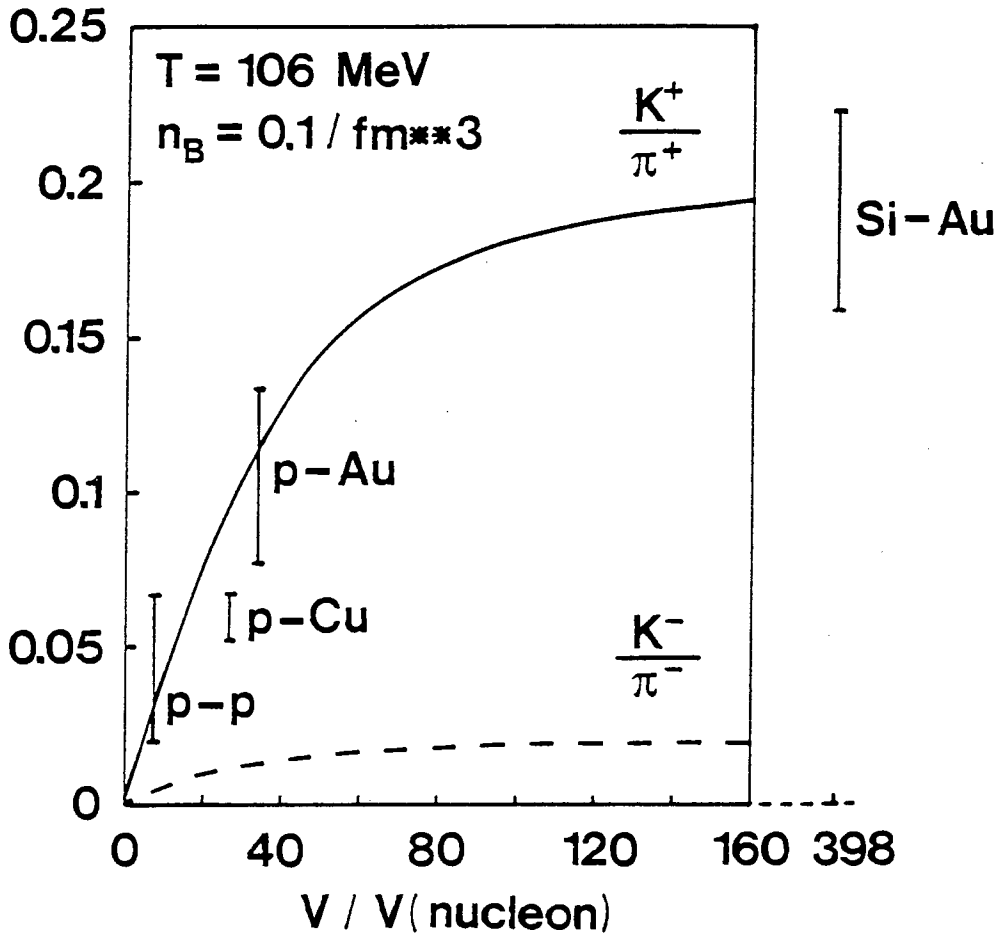

Figure 2.3: The K^+/π^+ and K^-/π^- ratios as a function of the interaction volume. The experimental points are plotted with their quoted error bars. Taken from [6].

the fact that massive resonances have more pions than kaons in their decay products, thus reducing the K^+/π^+ ratio. See Figure 2.5.

Consider now the abundance of strange baryons as measured recently by the NA35 and WA85 collaborations at CERN using a beam of sulphur ions at an energy of 200 GeV/nucleon. Figure 2.6 is a plot of the Ξ^-/Λ and the $\overline{\Xi^-}/\bar{\Lambda}$ ratios as a function of the baryon number B for a fixed net baryon density ($n_B = 0.1/\text{fm}^3$) and a fixed temperature T and using the exactly conserved baryon and strangeness formalism. The ratio as calculated in a gas containing all hadronic resonances up to a cut-off mass of approximately 1.6 GeV, (curve denoted 56) and for a gas composed of 124 hadronic resonances (including antiparticles), corresponding to a cut-off mass of about 2 GeV is presented. As can be seen from the figure the Ξ^-/Λ and the $\overline{\Xi^-}/\bar{\Lambda}$ ratios do not depend strongly on the hadronic resonances with masses above 1.6 GeV.

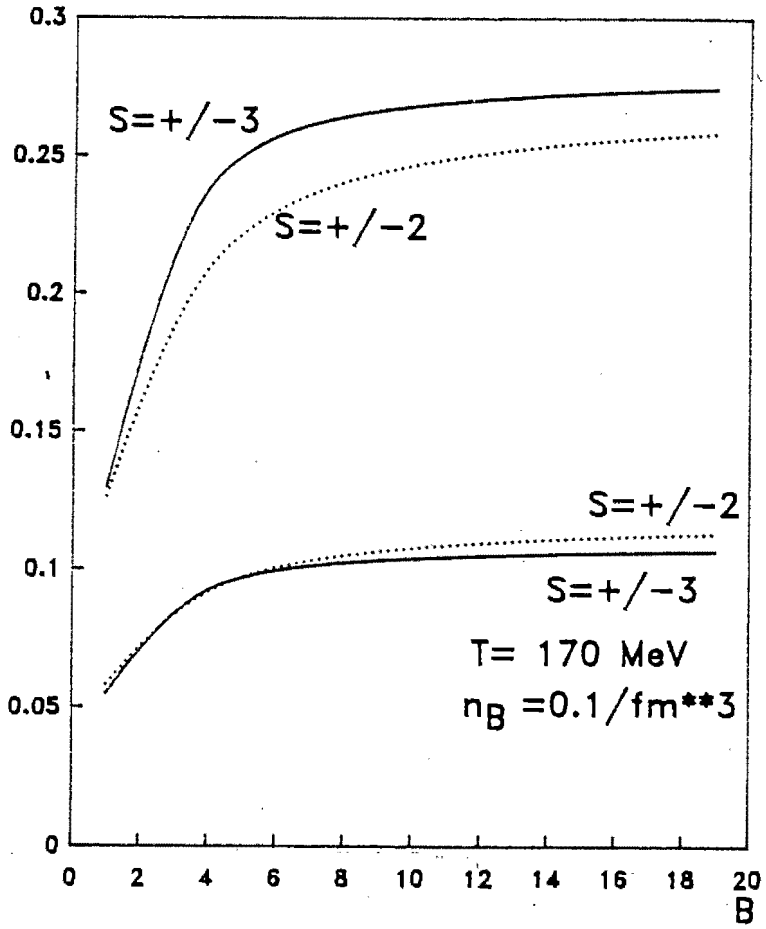

Figure 2.4: Comparison of K/π ratios derived from the $Z^2_{B,S}(T,V)$ and $Z^3_{B,S}(T,V)$ equations as a function of the baryon number B at fixed T and baryon density (0.1/fm^3).

For the $\bar{\Lambda}/\Lambda$ and the $\bar{\Xi}/\Xi$ ratios one finds the following: for small volumes the $\bar{\Lambda}/\Lambda$ ratio tends to zero because the Λ can be produced with one accompanying K while the $\bar{\Lambda}$ requires more accompanying particles in order to conserve strangeness as well as baryon number (e.g. ΛK versus $\bar{\Lambda}NN\bar{K}$). In a small system therefore the $\bar{\Lambda}/\Lambda$ ratio has to go to zero. This is not the case for the $\bar{\Xi}/\Xi$ ratio which approaches a finite value as the volume goes to zero. In this case the $\bar{\Xi}$ can be compensated by two Λ's ($N\bar{\Lambda}\bar{\Lambda}$) while the Ξ can be compensated by two kaons ($N\bar{K}\bar{K}$). From the formulae given in 1.1.2 one obtains ($S = 0$):

$$\lim_{V\to 0}\frac{\bar{\Xi}}{\Xi} \sim \lim_{V\to 0}\frac{I_2(2Z_Y)I_0(2Z_K)}{I_0(2Z_Y)I_2(2Z_K)}$$
$$\sim \left[\frac{Z_Y(T,V)}{Z_K(T,V)}\right]^2 = \left[\frac{m_Y^2 K_2(\frac{m_Y}{T})}{m_K^2 K_2(\frac{m_K}{T})}\right]^2$$

This is shown in Figure 2.7.

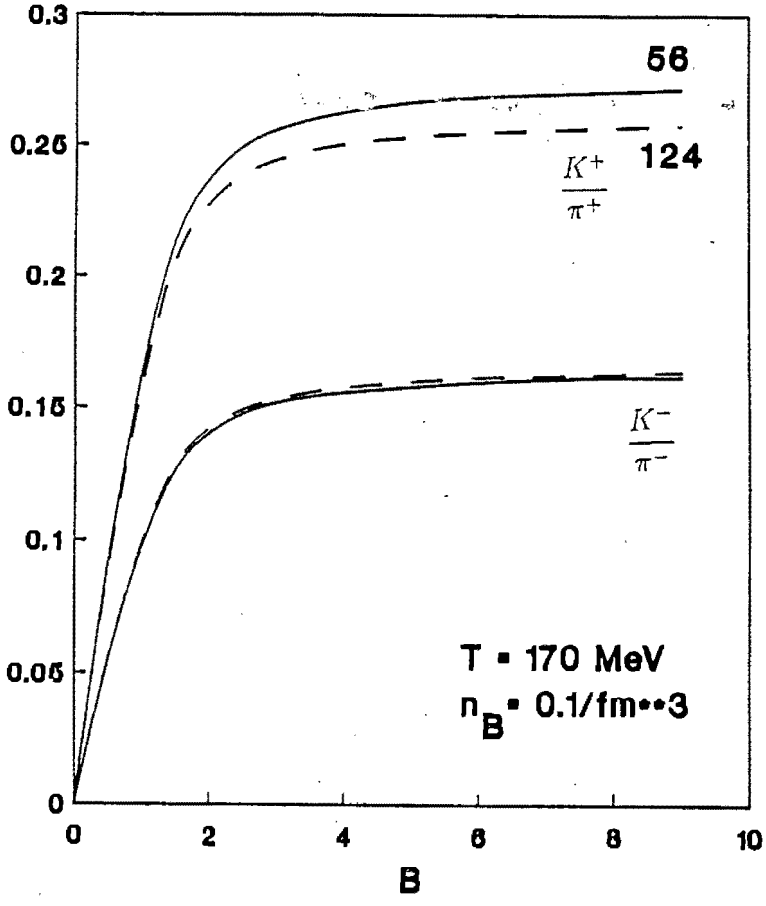

Figure 2.5: Comparison of K/π ratios derived from the $Z^2_{B,S}(T,V)$ equation as a function of baryon number B at fixed baryon density (0.1/fm^3) for different compositions of the hadronic gas: 56 and 124 resonances. Taken from [6].

Figure 2.8 and Figure 2.9 show the $\bar{\Lambda}/\Lambda$ and $\bar{\Xi}/\Xi$ ratios respectively. The curves labelled 5 have been calculated for a hadronic gas containing only the stable particles (K,N,Λ,Σ and Ξ) while the curves labelled 56 and 124 have been calculated for gases containing 56 (cutoff in mass approximately 1.6 GeV) and 124 (cutoff about 2 GeV) respectively. One sees that the results are substantially different in each case. This means that these ratios cannot be calculated reliably in this hadronic gas model. An independent calculation performed within the grand canonical ensemble showed the same trends: an increase in the number of resonances separates the ratios. Thus the number of hadronic resonances changes the results in a crucial way. This result can be explained most easily within the context of the grand canonical ensemble as follows. By increasing the number of hadronic resonances from 56 to 124 one also increases the net baryon number since baryons have a greater statistical weight

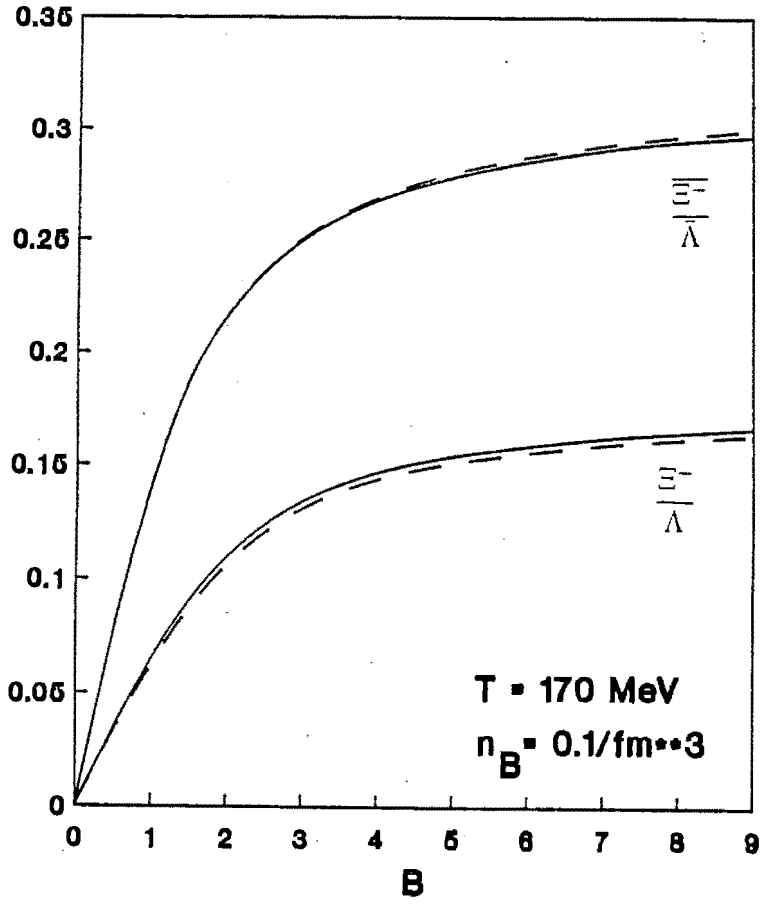

Figure 2.6: Ξ/Λ and $\overline{\Xi}/\overline{\Lambda}$ ratios as a function on baryon number B at fixed baryon density ($0.1/\mathrm{fm}^3$) for a gas composed of 56 and 124 resonances. Taken from [6].

than antibaryons because of the sign of the baryon chemical potential:

$$\begin{aligned} \text{baryons} &\sim \exp(-\frac{M}{T} + \frac{\mu_B}{T}) \\ \text{antibaryons} &\sim \exp(-\frac{M}{T} - \frac{\mu_B}{T}) \end{aligned}$$

However, the baryon density can only remain fixed in the system if one lowers the chemical potential μ_B. This in turn leads to a corresponding enhancement in the $\bar{\Lambda}/\Lambda$ and $\bar{\Xi}/\Xi$ ratios

$$\begin{aligned} \bar{\Lambda}/\Lambda &\sim \exp(-2\mu_B/T) \\ \bar{\Xi}/\Xi &\sim \exp(-2\mu_B/T) \end{aligned}$$

but not in the Ξ/Λ or K/π ratios since these are less sensitive to μ_B :

$$\Xi/\Lambda \sim \text{constant}$$

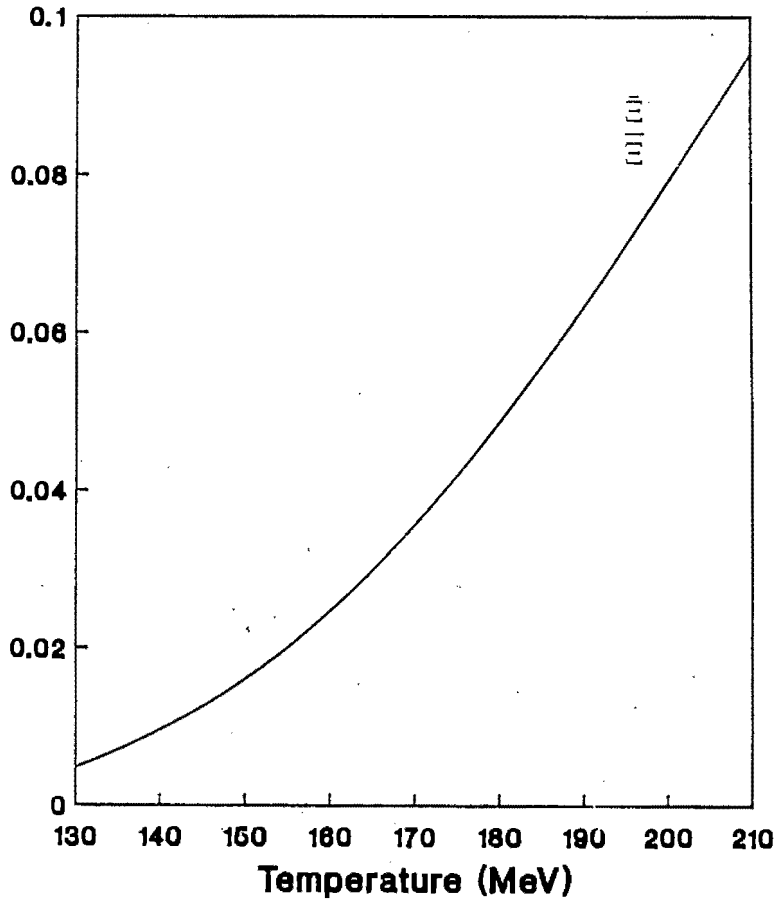

Figure 2.7: Small volume limit of $\bar{\Xi}/\Xi$ ratio for a gas composed of 56 resonances as a function of the temperature T. Taken from [6].

$$K/\pi \sim \text{constant}$$

Hence the observed behaviour seen in Figures 2.5 and 2.6 compared to the behaviour in Figures 2.8 and 2.9.

The final state of a relativistic heavy ion collision has been described by a hadronic gas with hard-core repulsion between particles. It has been found that for large baryon numbers and/or interaction volumes, a description using the grand canonical ensemble could be justified. For a small system, however, corrections arising solely from the exact conservation of baryon number and strangeness are important and cannot be neglected. This is particularly relevant if one wants to compare results from p-p collisions with those from heavy ion collisions. Most of the particle ratios considered ($K^+/\pi^+, K^-/\pi^-, \Xi^-/\Lambda, \overline{\Xi^-}/\bar{\Lambda}$ and $\bar{\Lambda}/\Lambda$) increase smoothly from zero in a small interaction volume towards the value obtained in the grand canonical ensemble. The only exception is the $\bar{\Xi}/\Xi$ ratio which tends to a finite

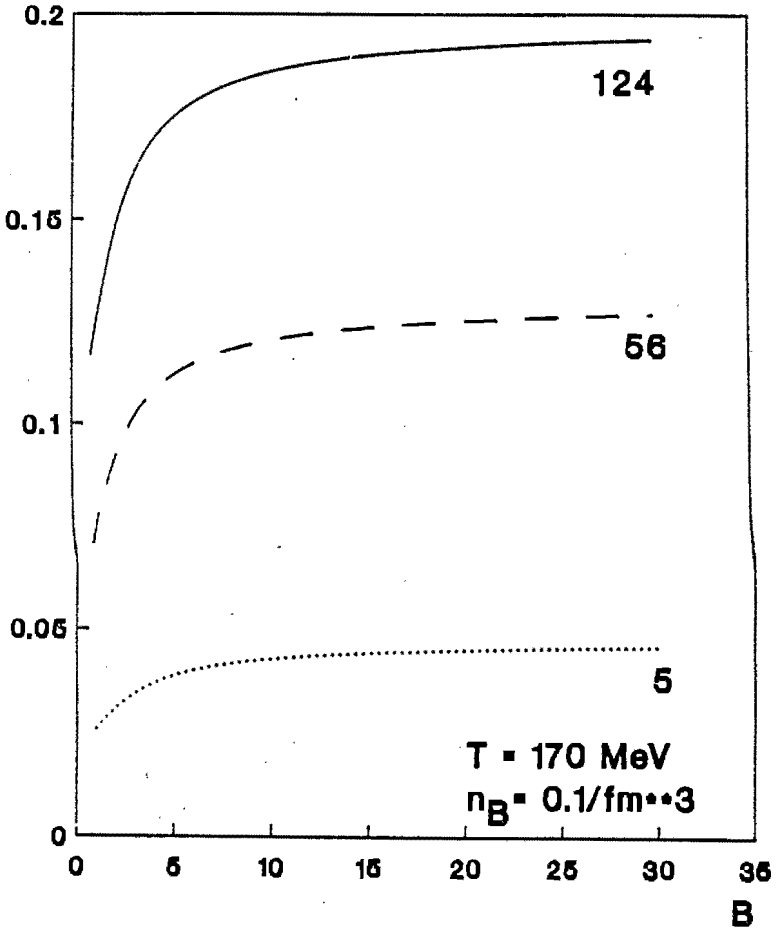

Figure 2.8: $\overline{\Lambda}/\Lambda$ ratio as a function of the baryon number B for three hadron gases containing 5,56 and 124 resonances at fixed temperature T and baryon density ($0.1/\mathrm{fm}^3$). Taken from [6].

non-zero limit for small interaction volumes.

Due to the dependence on the precise composition of the hadronic gas, i.e.the number of resonances kept, it turns out that the $\bar{\Lambda}/\Lambda$ and $\bar{\Xi}/\Xi$ ratios cannot be evaluated in a reliable manner at present. However, at some mass scale one hopes that these ratios saturate, that is, the Boltzmann factor $e^{\frac{-m}{T}}$ will at some point sufficiently suppress the heavier resonances and the $\bar{\Lambda}/\Lambda$ and $\bar{\Xi}/\Xi$ ratios can then be predicted independently of the number of resonances kept. Including resonances up to 2 GeV is clearly not sufficient. The determination of high mass resonances and their decay channels to date still poses an experimental challenge. The K/π ratios can be fitted reasonably well to the experimental data for p-p, p-Cu, p-Au and Si-Au collisions in a simple thermodynamical picture.

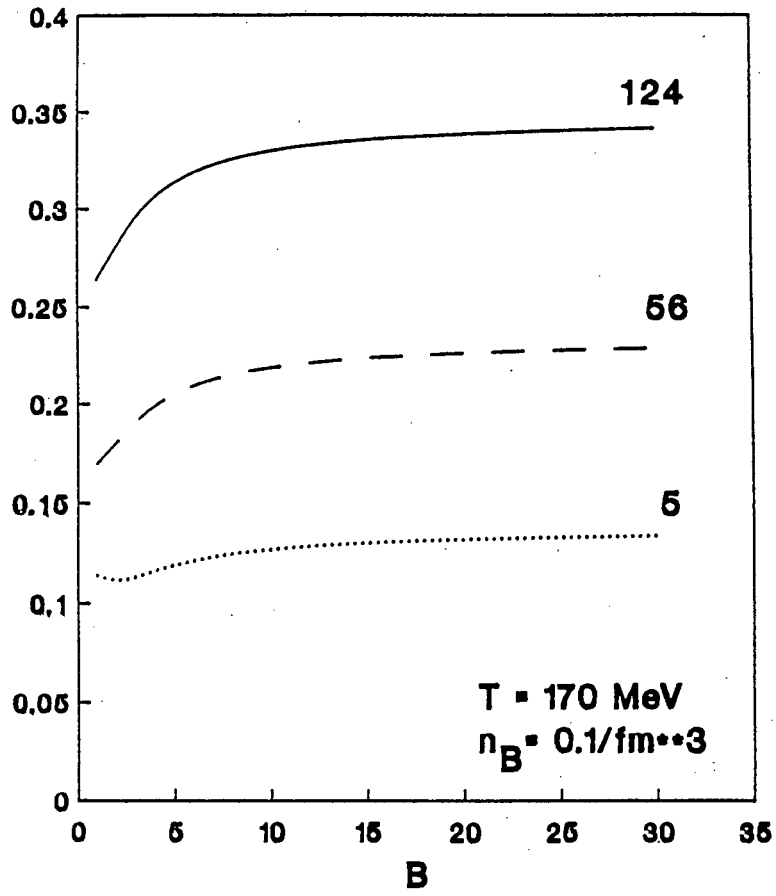

Figure 2.9: $\overline{\Xi}/\Xi$ ratio as a function of the baryon number B for three hadron gases containing 5,56 and 124 resonances at fixed temperature T and baryon density ($0.1/\text{fm}^3$). Taken from [6].

2.3 The Low-p_t π^- Anomaly

The transverse momentum (p_t) spectra of particles produced show a very interesting low- p_t charged pion enhancement leading to the question whether a new mechanism for low p_t π^- production is required.

Systematically, an increase in the charged pion multiplicity is observed when one increases $\sqrt{s}$ in p-p collisions. Experimentally, this increase has been established as being due to the resonances decaying into pions. The conclusion that one may draw is that resonance decay plays a major role to the π^--multiplicities, and thus perhaps also in nucleus-nucleus interactions. Note that the low-p_t roundoff in the π^- muliplicities is observed in the p_t-spectra and not in the transverse mass (m_t)-spectra. The so-called π^- anomaly has recently been discussed in [22]. For completeness the arguments are listed again.

The conclusions drawn by Sollfrank et al. come from comparing 2-body and 3-body decays. Less energy is available to the daughters in the 3-body decays and they thus tend to occupy the low-p_t region of the spectrum. Also, the 3-body decays exhibit clear thermal nature i.e. the plot of $m_t^{\frac{-3}{2}} dn/dm_t$ vs m_t is a straight line throughout whereas the line from the 2-body decays rounds off at low m_t. The authors also investigate the effect of finite width resonances on the p_t spectrum and find this effect to be small. By considering a hadronic gas of 11 resonances the authors were able to reproduce the experimental S-S data (NA 35) to within the error bars. The conclusion that can be drawn is that no new mechanism for π^- production is required at low p_t; the enhancement effect can be attributed to the resonances (these are thermal) which chiefly produce pions by 3-body decays. This argument is a strong contender to the proposed argument of nonequilibrium contributions to charged pion multiplicities [23]. Here the low-p_t pion enhancement is attributed to a partial thermal equilibration of a superdense pion fluid i.e. one having a greater density than predicted by assuming thermalisation. Modification of the pion p_t spectrum due to final state (elastic) $\pi\pi$ scattering leads to a nonzero pion chemical potential. Not only can the π enhancement be explained, but the spectral shift (dN/dp_t vs p_t) can also be reproduced accurately in the case of the NA 35 when making the assumption of partial thermalisation of the pions.
It is, however, satisfactory to know that equilibrium gas models at least do explain the low-π p_t behaviour simply by including enough resonances before one has to deal with nonequilibrium kinetic theory to explain the subtleties of the observed spectra.

2.4 Summarising Hadronic Gas Models

As has been demonstrated, hadronic gas models are a useful tool for describing the end products resulting from a collision. In their form they are simple to implement with all the parameters in principle obtainable from experiment.
The question on the type of ensemble to be employed has been discussed; for few-body collisions the canonical ensemble is required while for many-body physics the grand canonical ensemble suffices.
There are of course many ways in which to improve the hadronic gas models: including interaction terms, collective flow phenomena and possible nonequilibrium effects will surely refine the predictions but also add a number of parameters to the model. The question

whether the data measured can be understood in the simplest possible picture has been answered: up to problems with the number of resonances kept, the data is indeed compatible with a simple hadron gas model provided that one incorporates the finite volume of the hadrons and takes sufficiently many hadronic resonances into account.

Chapter 3

Thermodynamic Description of the Phase Transition

The phase diagrams obtained have been calculated with equilibrium (statistical) mechanical methods. It is important to understand whether or not the Gibb's criteria for the phase transition have to be modified when conserving quantum numbers as in our case, baryon number and strangeness. In this section the arguments given in [24] are developed again. In several of the papers to date the strange chemical potential suffers a discontinuous jump when going across the phase boundary from the hadronic phase to the quark gluon plasma. Since discontinuities lead to irreversible processes it seems neccessary to understand why these apparent discontinuities appear. The crucial observation to make is that both baryon number and strangeness have to be conserved globally i.e. in all regions of the phase diagram simultaneously. Conserving the quantum numbers locally will lead to discontinuities, as will be seen. (See for instance: [25],[36].)

Consider a two-phase system composed of quarks in phase 1 and hadrons in phase 2 in mechanical equilibrium. In order to model the non perturbative vacuum of the ground state of QCD a vacuum energy density of –B (B is the Bag Constant) is included in phase 1. The gluons allow the quarks to thermalise and their density is a function of the temperature only. The two phases are described by the following parameters and contain the following particles: phase 1 with volume V_1, energy E_1, quark numbers N_q, $N_{\overline{q}}$, N_s and $N_{\overline{s}}$. Phase 2 has volume V_2, energy E_2 and particle numbers N_N, $N_{\overline{N}}$, N_Λ, $N_{\overline{\Lambda}}$, N_K, $N_{\overline{K}}$ and N_π for the nucleons, lambdas, kaons and pions. The question is now whether one can determine the

particle numbers given the following constraints:

$$
\begin{aligned}
&S_1 + S_2 = S \text{ fixed total entropy} \\
&V_1 + V_2 = V \text{ fixed total volume} \\
&E_1 + E_2 = E \text{ fixed total energy} \\
&\frac{1}{3}(N_q - N_{\overline{q}}) + \frac{1}{3}(N_s - N_{\overline{s}}) + (N_n - N_{\overline{n}}) + (N_\Lambda - N_{\overline{\Lambda}}) = N_B \\
&\text{expressing baryon number conservation.} \\
&(N_s - N_{\overline{s}}) + (N_\Lambda - N_{\overline{\Lambda}}) - (N_K - N_{\overline{K}}) = -N_S = 0 \\
&\text{expressing strangeness conservation.}
\end{aligned}
\tag{3.1}
$$

Consider now the following reactions occuring at equal rates in chemical equilibrium as well as the reactions for the antiparticles:

$$
\begin{aligned}
q + q + q &\rightleftharpoons n \\
q + q + s &\rightleftharpoons \Lambda \\
q + \overline{s} &\rightleftharpoons K \\
q + \overline{q} &\rightleftharpoons \pi
\end{aligned}
\tag{3.2}
$$

If one were to conserve the quantum numbers in each of the phases separately one would restrict some of the above reactions which list the chemically allowed transfer of quarks to hadrons and vice versa.

The minimisation of the total energy of the system with respect to the entropy leads to the equality of temperature of the two phases and minimisation of the energy with respect to the volume yields the equality of pressure of the two phases at the phase transition point. The variations of the particle numbers take on the form:

$$
\sum_\alpha \mu_\alpha \, \delta N_\alpha + \sum_\beta \mu_\beta \, \delta N_\beta = 0 \tag{3.3}
$$

with the chemical potential μ as usually defined in thermodynamics. The label α runs over the quark species and label β over the hadronic species. Consider now the variations of the particle numbers. The question is whether they are compatible with the quantum number conserving relations expressed in equation (1) above or whether they are independent of them.

The variation of the particle numbers may be expressed as follows: (where τ runs over all contributing particle species)

$$\delta N_i = \sum_\tau \nu_{i\tau}\, \delta N_\tau \tag{3.4}$$

This equation states that the variation in the number of the ith species is brought about by the chemical (stoichiometric) coefficient $\nu_{i\tau}$ multiplied with the variation of the parent species N_τ summed over all allowed parent species. Note that the parent species are independent of another and must thus be varied independently. For example, one may consider the variation of the up and down quark species. This comes from a variety of reactions e.g. nucleon dissociation, lambda dissociation etc. Chemically, these reactions are independent of one another and occur at different rates.

If one subsitutes the varied particle numbers from (4) into (3) and uses the fact that different reactions are independent of one another then one obtains the chemical equilibrium condition for a given reaction:

$$\sum_\alpha \mu_\alpha\, \nu_{i\alpha} + \sum_\beta \mu_\beta\, \nu_{i\beta} = 0 \tag{3.5}$$

Note that this relation is independent of the parent species N_τ. If one considers the variation of the conserved charges, namely the baryon number and strangeness in a way similar to (4) one finds that they are also satisfied independently of the variations of the parent species. Consequently the conditions for equilibrium imposed by the chemical reactions are not affected by the imposition of the conservation equations since only the chemical coefficients appear and not the variation of the particle numbers (which are subject to the conservation laws).

The reverse of the above argument is as follows: one uses only the conservation equations with Lagrange multipliers which one can then eliminate in terms of equation (6). Thus the reaction equations do not produce any more restrictions to the conservation equations; all reactions are allowed that are not explicitly excluded by the conservation equations. The question is how the conservation equations manifest themselves in the system since we have shown that they do not alter the equilibrium conditions.

Consider now the problem of determining the equilibrium values of the variables listed in equation (1). The chemical potentials have specific relations in the quark and hadronic

phase:

$$\begin{aligned}
&\mu_q = -\mu_{\overline{q}} \ , \ \mu_S = -\mu_{\overline{S}} \\
&\mu_q = \frac{1}{3}\mu_B \\
&\mu_N = \mu_B \\
&\mu_B - \mu_S = \mu_\Lambda \\
&\mu_K = \mu_S \\
&\mu_\pi = 0.
\end{aligned} \tag{3.6}$$

The equality of pressure of the two phases allows one to eliminate one variable in terms of the others: (we choose to eliminate μ_S in terms of μ_B and T)

$$\begin{aligned}
&P_1(\mu_q, \mu_S, T) = P_2(\mu_B, \mu_S, T) \\
&\text{with } \mu_S = \mu_S(\mu_B, T)
\end{aligned} \tag{3.7}$$

The quantities V_1, V_2, μ_B and T are determined by the overall energy and volume conditions aswell as the conservation equations as listed in (1). The (zero) strangeness condition gives:

$$N_S = 0 = V_1 (n_{\overline{s}} - n_s) + V_2 (n_{\overline{\Lambda}} - n_\Lambda + n_K - n_{\overline{K}}) \tag{3.8}$$

Given the densities which are functions of the intensive variables μ_B and T one can solve the above equation for the ratio V_1/V_2 i.e.

$$\frac{V_1}{V_2} = f(\mu_B, T) \tag{3.9}$$

The total volume condition then specifies V_1 and V_2. The baryon conservation equation and the total energy condition then specify μ_B and T. All the variables have now been specified. The chemical equilibrium conditions establish relations among quantities and the conservation equations select certain values for some of these.

In summary, the two paramters μ_B and μ_S are coupled by the equality of pressure condition but are not modified by equilibrium conditions which in turn are not altered by the presence of the conservation equations. The discontinuities obtained for the strange chemical potential at phase transition to date are an artifact of preserving strangeness in each of the

phases seperately and not globally. When this is done consistently a coexistence region of nuclear matter and quark gluon plasma is found for particular values of the baryon chemical potential. The coexistence region is present for those values of the chemical potentials for which equation (8) yields a solution in the range (∞,0) for the ratio V_1 and V_2.

Chapter 4

The Physics of the Phase Transition

4.1 Prologue

The description of the deconfining phase transition of hadronic matter to the quark gluon plasma (QGP) is compactly described by thermalised gas models as an alternative to lattice gauge theory calculations. These are at present still restricted to the zero baryon density region as the calculations at finite baryon density are plagued by complex weights in the action $\mathcal{S}$. To date no conclusive techniques are available to eliminate this problem and thus extend the calculations of this fundamental theory to finite baryon density. Grand canonical gas models can be used to extrapolate from the zero baryon density point to finite baryon densities to investigate, for instance, the possible existence of condensates in the high baryon density region and the physics of the phase transition at zero temperature. Up to a short while ago these models suffered from a serious deficiency: they were thermodynamically inconsistent. This means that the ad-hoc changes introduced in order to realistically model the phase transition altered the thermodynamic relations in a way which prevented these modified relations from being directly derivable from standard thermodynamics. The problem was, of course, the question on how to include finite size effects in the (relativistic) theory. In order to understand why this was neccessary a brief historical review is of benefit.

At zero baryon density one expects a phase transition from a gas of mesons to a gas of asymptotically free quarks. In the simplest scenario a gas of massless pions undergoes a transition to a gas of massless u and d quarks. The pressure and density integrals can be calculated analytically (see Appendix 1) and one has the thermodynamic relation that

$P = \frac{1}{3}\epsilon$ where P is the pressure and ϵ is the energy density. Invoking the Gibbs' criteria for phase transitions in the grand canonical ensemble (thermal, chemical and mechanical equilibrium) one obtains a critical temperature T_c in the region 150 MeV $\leq T_c \leq$ 200 MeV for a range of the Bag Constant B 180 MeV$\leq$ B $^{\frac{1}{4}}$ $\leq$235 MeV. This rough estimate could be improved by including the gluon pressure, massive quarks, pions and α_s corrections.

In the massless limit one has that $P = \frac{1}{3}\epsilon$. However, the pressure of the quark gluon plasma is reduced by an amount –B relative to the vacuum which is taken to have zero pressure and the energy density increases by an amount B relative to the vacuum. Clearly the phase transition is first order in this model; the energy density jumps by an amount B when reaching T_c from the mesonic side. This is the latent heat required to vapourise pions into their consituent quarks.

The phase transition point at zero temperature can also be dealt with analytically. At this point only fermions and condensed bosons are present. As the treatment of relativistically condensed bosons is difficult it will be assumed that no condensation has taken place. The simplest picture of the phase transition from a gas of massless nucleons to a gas of massless quarks is unrealistic: from Appendix A the pressure of an ideal gas reads

$$P = \frac{g_i \mu^4}{24\pi^2}$$

Since $\mu_q = \frac{1}{3}\mu_b$ one finds that the hadronic pressure dominates everywhere; clearly this approximation is unrealistic. Turning to a massive fermion (nucleon) gas one finds that the pressure in the asymptotically large μ region reads

$$P_h = \frac{4\mu^4}{24\pi^2}$$

for the nucleons and for the u and d quarks the pressure reads:

$$P_q = \frac{12\mu^4}{24 \cdot 81\pi^2} - \mathrm{B}$$

Thus $P_h/P_q \rightarrow 27$ for sufficiently large baryon densities, contrary to what one expects from asymptotic freedom where one expects the quark phase to dominate [26].

For low baryon densities there is a region in which the quark phase has the higher pressure and is thus the favoured phase. This region is clearly a function of the Bag Constant B (usually taken independent of the baryon density and temperature T) and can be parametrized

as: (see [26],[27])

$$\frac{1}{2\pi^2}(\frac{m}{3})^4 \leq \mathrm{B} < (\frac{3}{8} - \frac{1}{2}\ln 2)\frac{m^4}{4\pi^2} \tag{4.1}$$

(m is the mass of the nucleon). The above equation corresponds to the following range in the value of $\mathrm{B}^{\frac{1}{4}}$: 149 MeV $\leq \mathrm{B}^{\frac{1}{4}} <$ 154 MeV which is a value of B close to the one obtained when fitting the baryon spectrum in the Bag Model ($\mathrm{B}^{\frac{1}{4}} = 145$ MeV is commonly used). The essential feature that is missing is that one has to include the volume of the hadrons (and mesons at finite temperature and chemical potential) since one expects the physics to change dramatically when the transition from a gas of extended particles takes place to a gas of pointlike Dirac particles- the quarks. How to take the volume of particles into account has a long history dating back to the classical Van der Waals equation of state but a relativistic counterpart has been notably absent in the literature.

A proposal motivated on geometrical grounds [26],[28],[29] is to reduce the total available volume by N times the volume of the particles. In the following discussion the only the "baryonic" variables will be changed i.e. only P_b and n_b will be modified. This is because the meson-meson crossection $\sigma_{\pi-\pi} \sim 25$ mb whereas the baryon-baryon crossection is significantly larger. Here N is the total number of baryons, to be replaced with the conserved quantity: $N_b - N_{\bar{b}}$ in the finite T region. Thus the equation for the density of pointlike baryons n_b^0 reads

$$n_b^0 = \frac{N_b}{V - NV_0} = \frac{n_b}{1 - n_b V_0} \tag{4.2}$$

where V_0 is the volume of the baryons. The above equation may be inverted to read for the extended baryon density n_b in terms of the (calculable) pointlike density n_b^0

$$n_b = \frac{n_b^0}{1 + n_b^0 V_0} \tag{4.3}$$

For deformable nuclei one should replace the volume V_0 by cV_0 where $c > 1$. Both the extended particle energy density and pressure are then given in terms of their pointlike counterparts by:

$$\epsilon_b = \frac{\epsilon_b^0}{1 + n_b^0 V_0}$$

and

$$P_b = \frac{P_b^0}{1 + n_b^0 V_0} \tag{4.4}$$

Asymptotically, the baryonic pressures and densities are given by

$$\begin{aligned} P_b &\sim \mu_b \\ n_b &\sim \frac{1}{V_0} \end{aligned} \tag{4.5}$$

The quark sector remains unchanged. The pressure and density here follow the usual trend:

$$\begin{aligned} P_q &\sim \mu_q^4 \\ n_q &\sim \mu_q^3 \end{aligned} \tag{4.6}$$

The problem of the hadronic phase returning at high densities (large μ) is now eliminated, albeit at the cost of thermodynamic consistency. Furthermore, the vanishing of the correction factors at zero μ means that the hadronic phase returns at sufficiently high temperatures. The basic thermodynamical relationship (valid in the thermodynamic limit)

$$\epsilon + P = \mu n + T s \tag{4.7}$$

neccessitates that:

- pressure is modified although no volume term appears in the expression for it in the infinite volume limit
- the modified particle density cannot be derived from the modified pressure:

$$n_b \neq \frac{\partial P}{\partial \mu_b}$$

- since the baryon number appears in the correction factor the hadronic phase will reappear at sufficiently high temperatures for $\mu = 0$.

This was the progress made up to 1986. It was known that both energy density and baryon number density were discontinuous at the critical temperature T_c and that a mixed phase of quarks and hadrons existing simultaneously in equilibrium was present when the phase diagram for nuclear matter was calculated. Furthermore, the bare-bones description of hadronic matter by pointlike physics was found to be intrinsically pathological.

$$\begin{aligned} P(T,\mu_B,\mu_S) &= P^0(T^0,\mu_B^0,\mu_S^0) \\ \mu_B &= \mu_B^0 + V_0\left[P^0(T^0,\mu_B^0,\mu_S^0) - P^0(T^0,0,0)\right] \\ \mu_S &= \mu_S^0 \\ T &= T^0 \end{aligned} \tag{4.9}$$

Note that the $-P^0(T^0,0,0)$ term is required in order to conserve baryon number at the phase transition: a hadronic gas at $\mu_B^0 = 0$ must go over into a quark gas at $\mu_B = 0$. We will now show in detail the consistency of the "baryonic" modification with the fundamental relations of thermodynamics, in particular with

$$\begin{aligned} dP &= s\,dT + n_B\,d\mu_B + n_S\,d\mu_S \\ \epsilon + P &= \mu_B\,n_B + \mu_S\,n_S + T\,s \end{aligned} \tag{4.10}$$

where the denotions ϵ, s, n_B and n_S are for the energy density, entropy density, baryon number density and strangeness, respectively.

- Baryon density

$$\begin{aligned} n_B &= \frac{\partial P}{\partial \mu_B} \\ &= \frac{\partial P}{\partial \mu_B^0}\frac{\partial \mu_B^0}{\partial \mu_B} + \frac{\partial P}{\partial \mu_S^0}\frac{\partial \mu_S^0}{\partial \mu_B} + \frac{\partial P}{\partial T^0}\frac{\partial T^0}{\partial \mu_B} \\ &= \frac{\partial P}{\partial \mu_B^0}\frac{\partial}{\partial \mu_B}[\mu_B - V_0 P] \\ &= n_B^0(1 - V_0 n_B) \end{aligned}$$

which leads to the well-known result

$$n_B = \frac{n_B^0}{1 + V_0 n_B^0}\,. \tag{4.11}$$

This is the expression which has been used for the corrected baryon density in references. Note that the baryon density appears and not the total particle density.

- Strangeness density

$$\begin{aligned} n_S &= \frac{\partial P}{\partial \mu_S} \\ &= \frac{\partial P}{\partial \mu_B^0}\frac{\partial \mu_B^0}{\partial \mu_S} + \frac{\partial P}{\partial \mu_S^0}\frac{\partial \mu_S^0}{\partial \mu_S} + \frac{\partial P}{\partial T^0}\frac{\partial T^0}{\partial \mu_S} \\ &= \frac{\partial P^0}{\partial \mu_B^0}\frac{\partial}{\partial \mu_S}[\mu_B - V_0 P] + \frac{\partial \mu_S^0}{\partial \mu_S} n_S^0 \\ &= n_B^0\left[-V_0\frac{\partial P}{\partial \mu_S}\right] + n_S^0 \\ &= -V_0 n_B^0 n_S + n_S^0 \end{aligned}$$

from which one obtains the strangeness density of extended particles:

$$n_S = \frac{n_S^0}{1 + V_0 n_B^0} \tag{4.12}$$

thus the change is the same as for the baryon density.

- Entropy density

$$\begin{aligned} s &= \frac{\partial P}{\partial T} \\ &= \frac{\partial P}{\partial \mu_B^0}\frac{\partial \mu_B^0}{\partial T} + \frac{\partial P}{\partial \mu_S^0}\frac{\partial \mu_S^0}{\partial T} + \frac{\partial P}{\partial T^0}\frac{\partial T^0}{\partial T} \\ &= \frac{\partial P^0}{\partial \mu_B^0}\frac{\partial}{\partial T}[-V_0 P] + \frac{\partial P^0}{\partial \mu_B^0}\frac{\partial}{\partial T} V_0 P(T,0,0) + s^0 \\ &= -n_B^0 V_0 s + s^0 + n_B^0 V_0 s^0(T^0,0,0) \end{aligned}$$

which leads to the result for the entropy density

$$s = \frac{s^0}{1 + n_B^0 V_0} + \frac{n_B^0 V_0}{1 + n_B^0 V_0} s^0(T^0,0,0) \tag{4.13}$$

An extra term appears this time proportional to the point-like entropy with vanishing chemical potentials.

- Energy density

It is now straightforward to extract the energy density. Inserting all the results obtained previously one obtains

$$\epsilon = \frac{\epsilon^0}{1 + V_0 n_B^0} + \frac{n_B^0 V_0}{1 + n_B^0 V_0} \epsilon^0(T^0,0,0) \tag{4.14}$$

i.e. similar to the entropy case.

Collecting all the changes one can show that the basic thermodynamic relation

$$-d\epsilon + T\,ds + \mu_B\,dn_B + \mu_S\,dn_S = 0 \tag{4.15}$$

is satisfied.

This concludes the discussion for the baryonic modification. The symmetrical modification

$$\begin{aligned} P(T,\mu_B,\mu_S) &= P^0(T^0,\mu_B^0,\mu_S^0) \\ \mu_B &= \mu_B^0 + V_0\left[P^0(T^0,\mu_B^0,\mu_S^0) - P^0(T^0,0,0)\right] \\ \mu_S &= \mu_S^0 + V_0\left[P^0(T^0,\mu_B^0,\mu_S^0) - P^0(T^0,0,0)\right] \\ T &= T^0 \end{aligned} \tag{4.16}$$

yields a similar correction factor for the baryon, strangeness, entropy and energy density (as well as being thermodynamically consistent) with the slight modification that the overall correction factor:

$$\frac{1}{1+n_B^0 V_0} \rightarrow \frac{1}{1+(n_B^0+n_S^0)V_0} \tag{4.17}$$

The entropy density (equation (13)) gets an extra term in the numerator of the second piece:

$$n_B^0 \rightarrow n_B^0 + n_S^0 \tag{4.18}$$

A similar correction is needed in equation (14) . Equation (15) is satisfied identically.

The phase diagrams discussed in the later sections have all been calculated at zero strangness i.e. the gas had $\langle S\rangle = 0$ so there is no immediate change in the correction factor but because the strange chemical potential of the quark sector is boosted by a term proportional to the hadronic pressure, the physics will be very different.

4.4 Phase Diagram with Modified Chemical Potentials

The phase diagrams presented were obtained by considering a mixture of a relativistic Bose and Fermi gas. Each particle carrying either baryon number and/or strangeness was assigned the same hard core radius $R = 0.8$ fm corresponding to a hard- core volume $V_0 = 2.14$ fm^3.

In the quark sector a value of 235 MeV was used for $B^{\frac{1}{4}}$. The equation of state thus obtained is quite hard: the particles continue to occupy a rather large volume, even when large compression takes place. Since the modified chemical potentials contain only the repulsive effect it is clear that the equation of state obtained is valid only for the high T and large μ limit, precisely because the attractive interactions leading to bound states are ignored. At this stage the reader is referred to the chapter "Thermodynamic Description of the Phase Transition" where it is shown that in order to correctly construct the phase diagram for a system with the two conserved charges baryon number and strangeness, it is neccessary to parametrize the strangeness content of the gas in the form:

$$n_S = \alpha\, n_{S,Q} + (1-\alpha)\, n_{S,H} = 0 \tag{4.19}$$

where $\alpha = V_Q/V$ i.e. the volume fraction of the quark sector compared to the volume of the system. The phase diagram corresponding to $\alpha = 0$ (the hadron boundary) and $\alpha = 1$ (the quark boundary) are shown. Note that the label **HG** refers to the hadron gas phase and the label **QGP** refers to the quark gluon plasma phase in the plots. For other values of α the reader is referred to reference [34]. With this in mind we can turn to the phase diagrams presented.

The diagrams corresponding to the modification of only the baryonic chemical potential (that is, the strange chemical potential is left at its point-like value μ_S^0) are consistent with the by now established expectations:

- no mixed phase at $\mu_B^0 = 0$ as predicted from lattice calculations
- kaon condensation occurs at low temperatures ($T < 80$ MeV) and at high baryon densities ($\sim$ twice nuclear matter density). (See Section 4.5 for a discussion of the effect of Bose-Einstein condensation of kaons.) (Figure 4.2,4.3)
- kaon condensation occurs only in the mixed phase where most of the hadrons ($\sim 90\%$) are already converted to quark matter [35],[34].
- a coexistence region in μ_S^0 of quarks, gluons and hadrons attributable to strangeness conservation [24].(Figure 4.2)

The diagrams corresponding to the shift of all the chemical potentials are also shown. There are several important similarities and differences to the previous results:

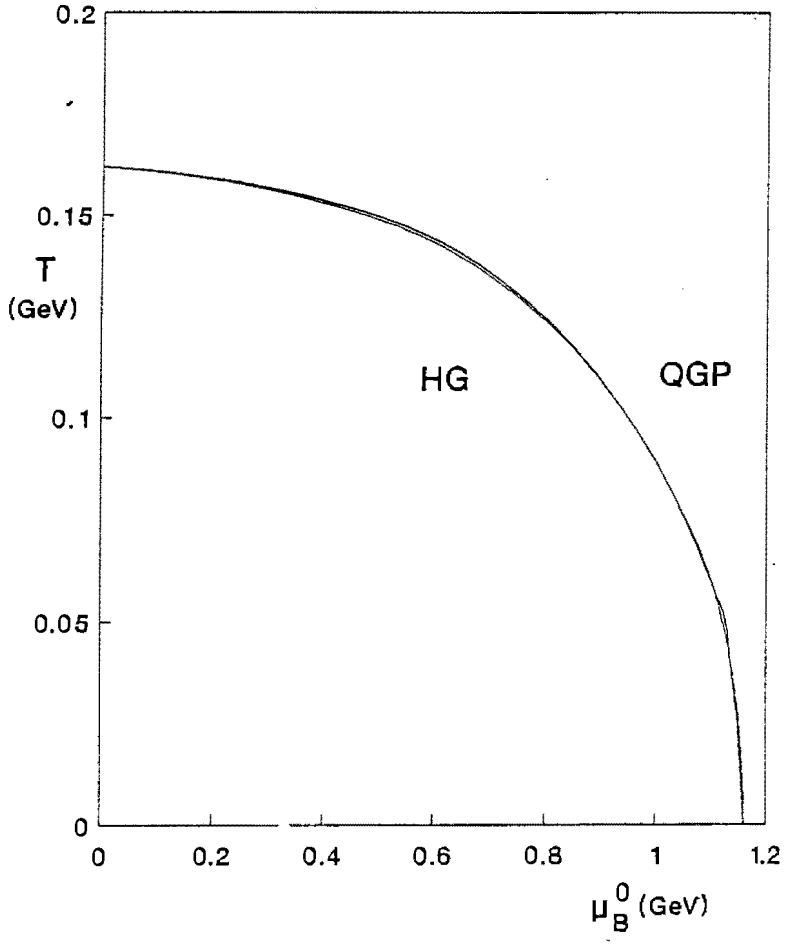

Figure 4.1: T vs μ_B^0 plot for case where only μ_B is shifted. No coexistence region because of baryon number conservation. Curve shown is the phase boundary between hadronic gas and quark gluon plasma.

- again no mixed phase at $\mu_B = 0$.

- kaon condensation (which depends on the value of the pointlike strange chemical potential $\mu_S^0 = m_K$) is not manifest at all. This is because the strange chemical potential of the quark phase is given a boost proportionally to the hadronic pressure. From the equality of pressure condition of the two phases this requires a smaller μ_S^0 in the hadronic phase, less than is required for kaon condensation.

- the strange chemical potentials across the phase boundary are switched, i.e. in both the cases of T vs. μ_S^0 and T vs. μ_S the chemical potential of the hadron gas is greater than that of the quark gluon plasma. The point to note is that the calculations in the hadronic phase are done with point-like chemical potentials whereas the calculations

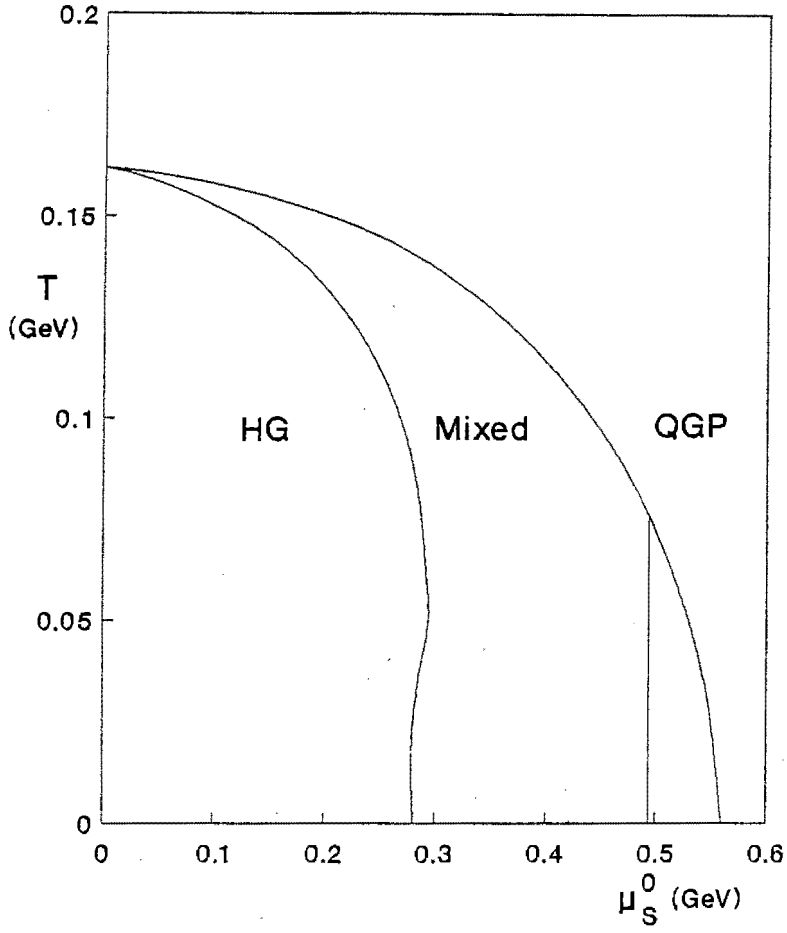

Figure 4.2: T vs μ_S^0 plot showing coexistence region "(Mixed)" where hadrons, quarks and gluons are present simultaneously in thermodynamical equilibrium and showing the region where Bose-Einstein condensation of kaons can take place. (To right of vertical line which defines the onset of condensation at $\mu_S^0 = m_K$.)

in the QGP are performed with shifted values of μ. There are thus no problems with the Gibbs' criteria being fulfilled. The T vs. μ_B and T vs. μ_B^0 curves show the correct behaviour. See Figure 4.4 and Figure 4.5 for details.

- the mixed phase is as pronounced for μ_S and μ_S^0 in this formalism as it is for the case where only one chemical potential is shifted; of the order $\sim$ 200 MeV broad at $T = 0$. See Figure 4.4 and Figure 4.5.

The diagrams obtained are in good agreement with most of those found in the literature [36],[37]; the important feature is the existence of a large mixed phase which does not disappear when all chemical potentials are shifted symmetrically.

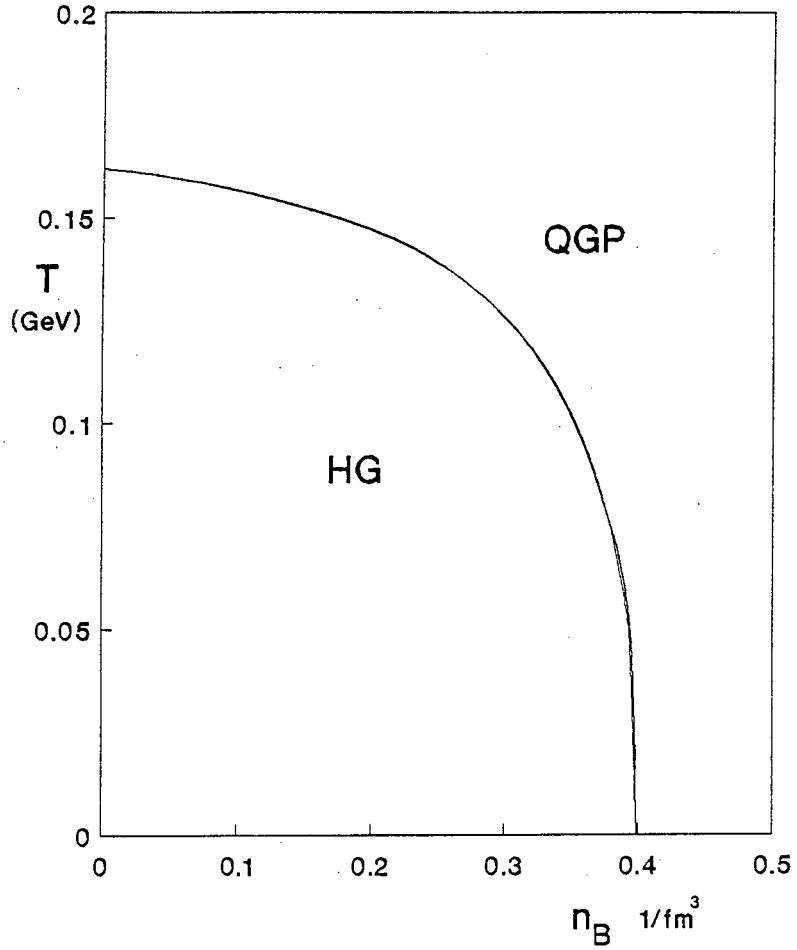

Figure 4.3: T vs n_B plot showing the baryon density at the phase transition. For the case where only μ_B is shifted from its pointlike value.

4.5 Bose-Einstein Condensation of Kaons

The question of Bose-Einstein condensation of kaons has been hotly discussed for several years now. Indeed, the condensation of free bosons has never been observed [2], so the possible existence of a relativistic condensate is even more intriguing.

Bosons can condense into the zero momentum mode because of their positive statistical correlations: unlike fermions which repel another, bosons tend to clump together [38]. The singular nature of the Bose-Einstein distribution at $p = 0$ and $\mu = m$ (here m is the mass of the boson) signals the phase transition. Condensation can only take place in the presence of a conserved charge, generally of U(1) symmetry, e.g. strangeness if one has chemical equilibrium.

In the literature one usually finds a discussion of the nonrelativistic Bose-Einstein conden-

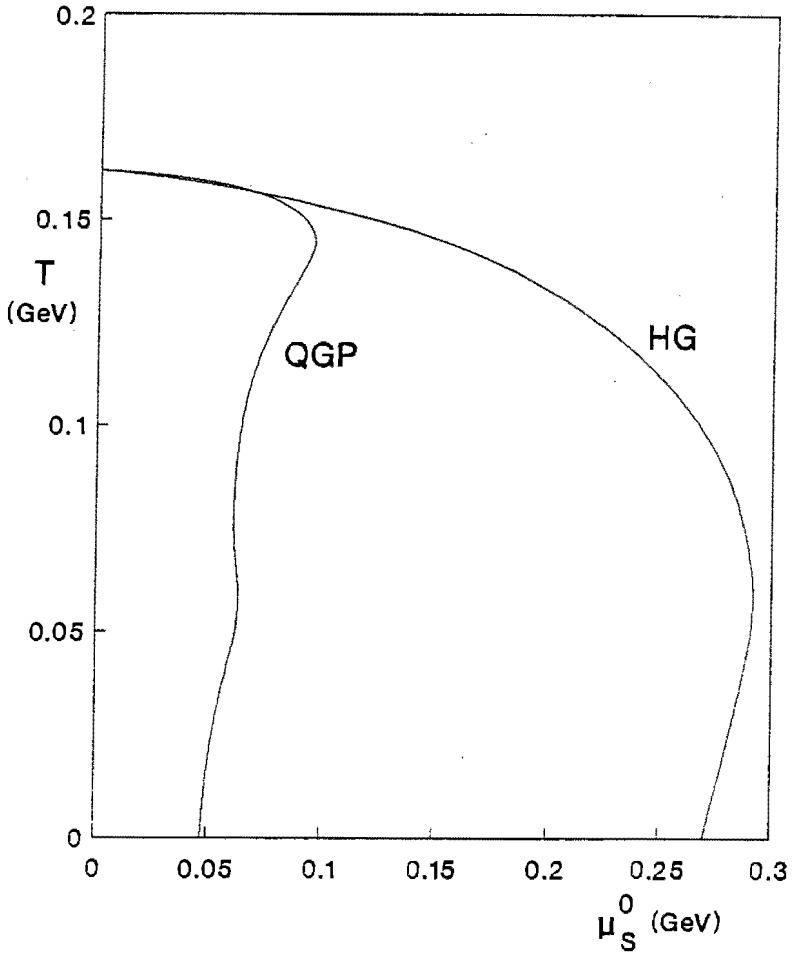

Figure 4.4: T vs. μ_S^0 plot for the case where both chemical potentials are shifted. Note that μ_S^0 for the hadron phase is larger than that of the plasma at the phase transition. Note that no condensation of kaons takes place.

sation [38] which is determined by the restriction that $m \gg T$ where T is the temperature. The expression for the ground state charge density Q_0 is

$$Q_0 = Q\left[1 - \left(\frac{T}{T_c}\right)^{\frac{3}{2}}\right] \tag{4.20}$$

where T_c is the temperature determined by

$$Q = V\int \frac{d^3p}{(2\pi)^3}\frac{1}{\exp\left(\frac{p^2}{2mT_c}\right) - 1} \tag{4.21}$$

In the relativistic scenario the integrals for the conserved charge slightly more complicated: the nonrelativistic energy-momentum relation $E = p^2/2m$ is replaced by the relativistic one: $E = \sqrt{p^2 + m^2}$. In the region where $T_c \gg m$ one finds that the critical temperature T_c is

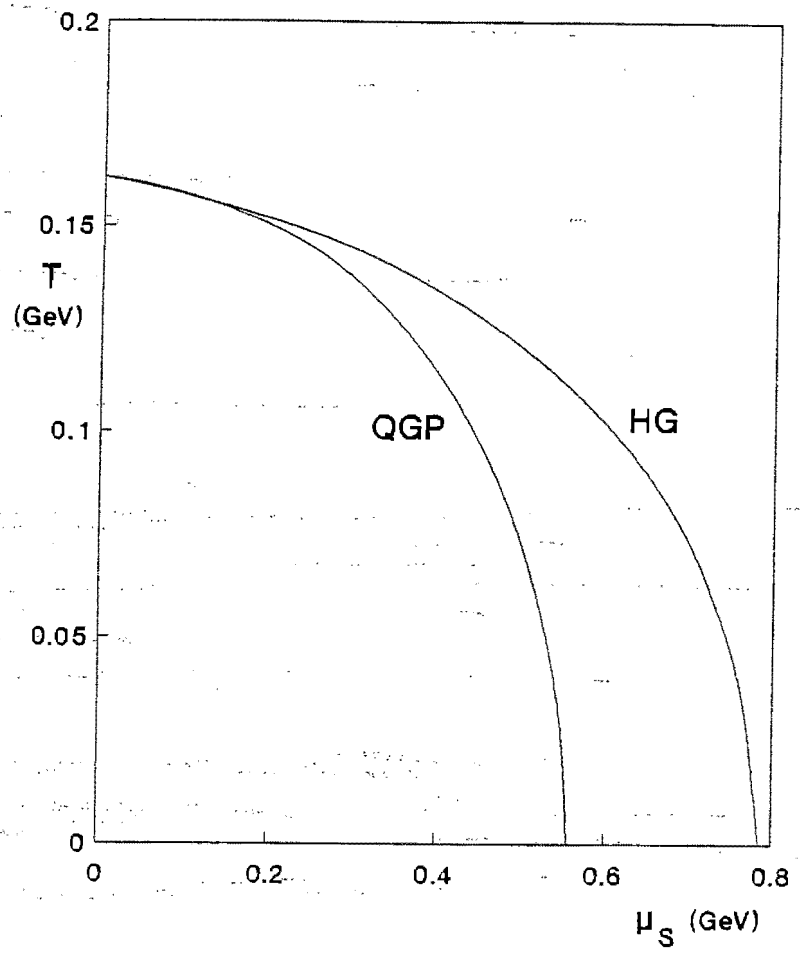

Figure 4.5: T vs. μ_S plot showing coexistence region. μ_S for the hadronic phase is again larger than in the quark phase because the potentials are shifted proportionally to the hadronic pressure.

determined by

$$T_c \simeq \sqrt{\frac{3|Q|}{mV}} \tag{4.22}$$

Below T_c the charge density in the ground state is given by (see [39],[40])

$$Q_0 = Q\left[1 - \left(\frac{T}{T_c}\right)^2\right] \tag{4.23}$$

Bose-Einstein condensation of kaons has been discussed in the literature for some time now, see [36],[41],[42],[43],[44]. The questions raised are:

- is condensation model dependent?
- if so, where does it take place? Before or after the transition to the QGP?

- how can it be seen; what are the experimental signatures?

Kaon condensation in the free-gas model was proposed by Cleymans et al. in [36]. The point to note was that the proposal made by the authors that kaon condensation takes place in extremely dense nuclear matter at low temperatures was founded on thermodynamically inconsistent volume corrections. These corrections were of the type discussed in the prologue. With these type of corrections it is clear that condensation has to take place at some stage: correcting the hadronic pressure results in an increase in μ_B which in turn causes μ_S to reach the kaon mass and signal the onset of condensation.

Note that for $\mu_B > 0$ there is a baryon-antibaryon asymmetry which results in an excess of strange baryons. This excess of strange baryons can only be counteracted by an increase in the number of antistrange mesons, hence K^+ condensation for the case where the overall strangeness of the gas is zero. The baryon chemical potential and strange chemical potential are coupled, see the previous chapter.

The first question has recently been discussed by Davidson et al. in [43]. They proposed a thermodynamically consistent mean field model where baryon-baryon and meson-meson interactions were included in the Hartree approximation, that is, self energy contributions were included by modifying the free space dispersion relation

$$E = \sqrt{p^2 + m^2} \rightarrow E = \sqrt{p^2 + m^2} + k_M n_M$$

where k_M and n_M are the meson-meson coupling strength and meson density, respectively [43]. Similar terms were used for the baryons. The authors chose values for the coupling strengths and showed that condensation does not take place. Again, the coupling strengths were taken from nuclear physics, that is physics at low temperatures and densities. How these parameters change when going to dense media is an important consideration. One set of parameters was chosen and used throughout, no comparisons using other parameters were made in the paper. Thus the existence of a condensate cannot be excluded outright; it seems to depend on the form of the hadronic interactions.

The phase diagrams constructed with the modified potentials again point out this model dependence: shifting only μ_B^0 (which results in a correction factor of $(1+V_0 n_B^0)^{-1}$) leads to a condensate whereas the quantum number modification (which leads to a correction factor of $(1 + V_0(n_B^0 + n_S^0))^{-1}$) does not show a condensate, although some other peculiar properties:

the strange chemical potentials are "inverted" at the phase transition; μ_S^0 and μ_S for the hadronic phase is greater than the corresponding terms for the quark gluon plasma. This is because the strange quark pressure is boosted proprtionally to the hadronic pressure thus μ_S^0 and μ_S have to decrease to fulfil the requirement of equality of pressure at the phase transition point. However, it should be noted that μ_S^0 which is used in the hadronic phase is always less than μ_S which is used in the quark phase.

A common observation ([34],[35],[36]) is that kaon condensation, should it take place, occurs at low temperatures and very high baryon densites, of the order 3-4 times nuclear matter density. Thus the analysis of Haber et al. [39] of high-T condensation does not apply here. It makes more sense to speak of induced condensation; induced because of the interplay of two quantum numbers, the baryon number and strangeness. Thus the study of a fixed charge canonical Bose-Einstein and Fermi-Dirac gas of, say, kaons and lambdas, might shed light on how Bose-Einstein condensation is induced by varying the density of the baryons. Following the prescription and the notation of Section 1.2 this partition function reads:

$$\begin{aligned} Z_{B,S}(T,V) &= \frac{1}{2\pi}\int_0^{2\pi} d\psi \exp(-iB\psi)\frac{1}{2\pi}\int_0^{2\pi} d\phi \exp(-iS\phi) \\ &\exp\left[V\int\frac{d^3p}{(2\pi)^3}(\ln(1+\exp(-E/T+i(\psi-\phi)))+\ln(1+\exp(-E/T-i(\psi-\phi))))\right] \\ &\exp\left[-V\int\frac{d^3p}{(2\pi)^3}(\ln(1-\exp(-E/T+i\phi))+\ln(1-\exp(-E/T+i\phi)))\right] \end{aligned} \tag{4.24}$$

In the calculations with only μ_B^0 shifted it was observed that kaon condensation sets in. This occurs when $\mu_S = m_K$. At that point an increase in the strange chemical potential is no longer possible otherwise the density of the kaons could become negative. Thus once the strange chemical potential reaches the kaon mass, the hadronic phase stagnates; it cannot exist for $\mu_B > m_K + \mu_S$. Thus unless the hadronic phase changes to quark matter at that point, it can never do so.

The alternative is to introduce a kaon-kaon interaction (repulsive) of the type $\mathcal{L} = -\lambda(\Psi_K^\dagger\Psi_K)^2$ where Ψ_K is the kaon field and λ a measure of the repulsive interaction. The minimum value of λ is determined by the electromagnetic coupling strength, ~ 1. Treating the kaons in the mean field approach, that is, only the condensed kaons interact with each other, leads to a contribution of the condensed kaons to the pressure and density of the form:

$$P_{\text{condensed}} = \frac{1}{4\lambda}(\mu_K^2 - m_K^2)^2 \qquad (\mu_K > m_K) \tag{4.25}$$

and

$$\begin{aligned} n_{\text{condensed}} &= \frac{1}{\lambda}(\mu_K^2 - m_K^2)\,\mu_K \qquad (\mu_K > m_K) \\ &= 0 \qquad\qquad\qquad\qquad (\mu_K < m_K) \end{aligned} \tag{4.26}$$

The derivation of these results can be found in [35]. In this way the chemical potential of the kaons can exceed the rest mass of the kaons and the phase diagram can be completed; it is thus also a type of mean field model. For an investigation how the phase diagram changes as a function of λ, see [34].

The phase diagrams found on the previous pages were constructed with $\lambda = 100$.

Thus one finds that, if condensation takes place, it occurs at high densites and low temperatures. A signal for the effect would be an increase in the number of correlated kaons at low p_t.

4.6 Further Comments on Modified Quantum Number Potentials

Several interesting results concerning the strange chemical potential can be derived by considering the low temperature region of the phase diagram. At $T = \tau$ such that $\tau \ll m$, the average zero strangeness of the gas requires that the density of the lambdas is equal to that of the kaons (the K^+'s and K^0's). For the case where $\mu < m$ i.e. the Λ's are produced only thermally one finds that, by equating the Boltzmann densities (see [25]):

$$\begin{aligned} n_\Lambda &= \frac{g_\Lambda}{(2\pi)^3}\int d^3p \exp\left(\frac{-(E_\Lambda - \mu_B^0 + \mu_S^0)}{\tau}\right) \\ &= \frac{g_K}{(2\pi)^3}\int d^3p \exp\left(\frac{-(E_K - \mu_S^0)}{\tau}\right) \\ &= n_K \end{aligned} \tag{4.27}$$

Since $T = \tau \sim p$ one has that $E_i \simeq m_i$ and thus truncating the integral at the $p = 0$ point leads to the following equation:

$$\mu_S^0 = \frac{1}{2}(\mu_B^0 - m_\Lambda + m_K) \tag{4.28}$$

This equation still holds if one shifts both potentials in a symmetric way. In the mixed phase the strangeness neutrality is guaranteed by a balance of the K^+ and s-quark density. By a

similar argument to the one above one finds that the chemical potential μ_S is, at $T = \tau$, given by

$$\mu_S^0 = \frac{1}{2}(m_K - m_s + \frac{\mu_B}{3}) \tag{4.29}$$

Two comments are in order. The above holds if $\mu_S < m_K$ otherwise kaon condensation sets in, $\mu_\Lambda < m_\Lambda$ is required for Boltzmann statistics and furthermore it holds only for the case $\mu_S = \mu_S^0$. For the case where both potentials are shifted this equation reads

$$\mu_S^0 = \frac{1}{2}\left[(m_K - m_s + \frac{\mu_B}{3}) - V_0\left(P(T^0, \mu_B^0, \mu_S^0) - P(T^0, 0, 0)\right)\right] \tag{4.30}$$

This is the low T point –dictated by overall strangeness neutrality– to which all the curves of constant volume fraction α (except $\alpha = 0, 1$) tend.

In summary then, there are 3 points at $T = \tau$ to which the strange chemical potential is restricted: (the first row of each item corresponds to the case where $\mu_S = \mu_S^0$, the row set in brackets to the case where the strange chemical potential is modified similarly to the baryon chemical potential.

- (1) $\alpha = 0$ $\mu_S^0 = \frac{1}{2}(\mu_B^0 - m_\Lambda + m_K)$
  $\left[\mu_S^0 = \frac{1}{2}(\mu_B^0 - m_\Lambda + m_K)\right]$
- (2) $0 < \alpha < 1$ $\mu_S^0 = \frac{1}{2}(m_K - m_s + \frac{\mu_B}{3})$
  $\left[\mu_S^0 = \frac{1}{2}(m_K - m_s + \frac{\mu_B}{3}) - \frac{1}{2}V_0\left(P^0(T^0, \mu_B^0, \mu_S^0) - P^0(T^0, 0, 0)\right)\right]$
- (3) $\alpha = 1$ $\mu_S^0 = \frac{\mu_B}{3} - m_s$
  $[\mu_S^0 = \frac{\mu_B}{3} - m_s - V_0\left(P^0(T^0, \mu_B^0, \mu_S^0) - P^0(T^0, 0, 0)\right)]$

Although the results obtained are in good agreement with those in the literature, one problem remains with the quantum-chemical formulation: since the correction factor $(1 + V_0 n_B^0)^{-1}$ vanishes at zero baryon chemical potential, it is of the same form as the ad-hoc modification discussed in the prologue. The problem of the hadronic phase (strictly the mesonic) returning for high T is recurrent. This is demonstrated in the P vs. T^4 plot, Figure 4.6.

At low T the hadronic phase dominates, in the intermediate temperature range of 162 MeV $\leq T \leq$ 300 MeV the quark phase dominates but then the hadronic phase returns, contrary to what one expects. The origin of this problem can be traced back to the rapidly increasing multiplicity of the hadronic phase as a function of temperature whereas the multiplicity of

the quark phase is fixed at the number of quark flavours. The vanishing of the correction factors at $\mu = 0$ is a feature of the quantum chemical formulation.

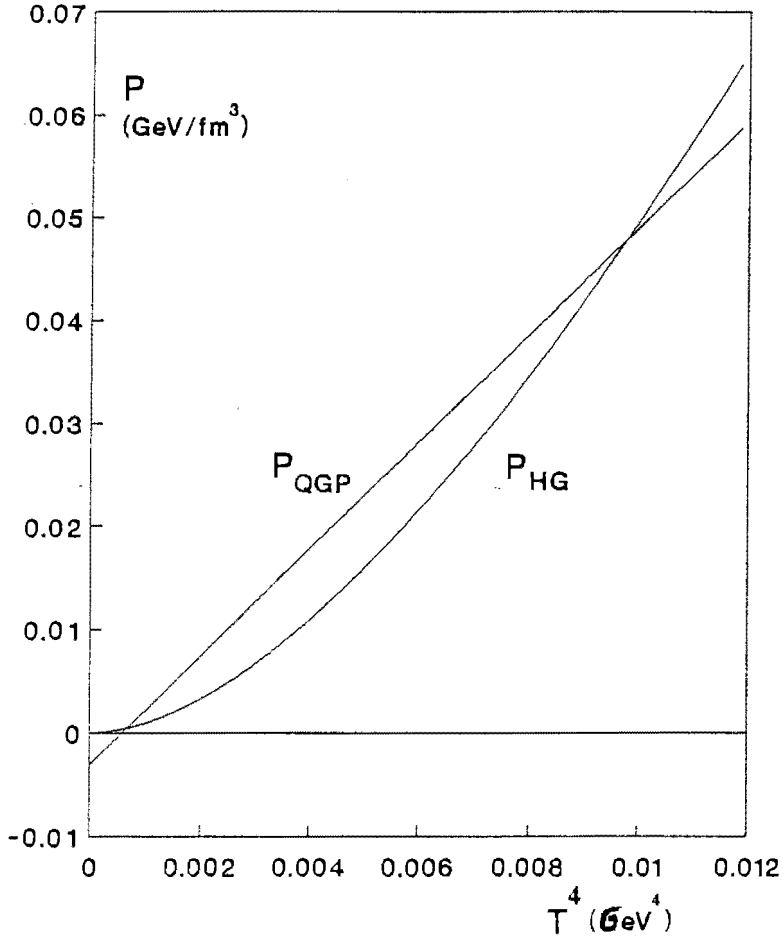

Figure 4.6: The pressure P vs T^4 at μ_B=0 in the modified chemical potential formalism. Only μ_B has been shifted from its pointlike value μ_B^0. The hadronic phase is seen to reappear at high T.

As a concluding remark it should be stressed that the concept of a relativistically rigid body of fixed volume V_0 is not correct; it violates causality. However, at the temperatures the phase transition is expected to occur the particles are non relativistic and this effect is not expected to play a major role.

4.7 Interacting Plasma with Consistent Volume Corrections

The calculations performed with the thermodynamically consistent corrections are at best still a very naive picture of the highly complicated physics of the phase transition of hadronic into quark matter. Interactions in the plasma have been ignored from the beginning. Hadronic

interactions have been assumed to be only repulsive and all hadrons were endowed with the same hard core volume. However, that the quark masses were taken to be zero (except the s-quark) does make sense when dealing with very dense media: asymptotic freedom allows

A modification of our model which would cure the μ=0 problems is to include quark-gluon interactions in the plasma [45]. The hadronic side of the phase diagram has been modelled taking into account the neccessary features at high density: volume. The strong coupling constant α_S which is a momentum, temperature and renormalisation dependent quantity should ideally be used to represent the quark-gluon interactions. Although calculations have been performed with nonzero α_S, the important feature of the coupling constant is its explicit temperature dependance.

The inclusion of a α_S term of the form

$$\alpha_S(Q^2) = \frac{4\pi}{(11 - \frac{2}{3}N_f)\ln\left(\frac{Q^2}{\Lambda^2}\right)} \tag{4.31}$$

(where Λ is the renormalisation scale set at a few hunderd MeV, Q^2 is the four momentum transfer of the scattering process and N_f the number of quark flavours) yields a correction to the pressure of the QGP of the form (for two massless quark species)

$$P_{\mathrm{QGP}} = P_{\mathrm{ideal\ QGP}} - \alpha_S\left(\frac{11}{9}\pi T^4 + \frac{2}{\pi}{\mu_q}^2T^2 + \frac{{\mu_q}^4}{\pi^3}\right) \tag{4.32}$$

Uddin and Singh [46] show that unless one includes terms up to order g^3 the pressure of the QGP at low temperatures $\sim$ 50 MeV becomes (unphysically) negative. Furthermore they show that α_S varies strongly in the region $T \sim 150$ MeV which is the temperature region where the problems of the recurring hadronic phase occurs at $\mu = 0$. Thus including higher orders in the coupling constant is vital. However, in this region ($T \sim \Lambda$) perturbation theory becomes unreliable and lattice gauge techniques are neccessary.

The following conclusions can thus be drawn: including temperature dependent α_S corrections to the QGP is an important feature which could prevent the hadronic phase recurring at μ=0. This is because the $\mathcal{O}(g^3)$ term is additive to the pressure, enhancing the QGP pressure, not reducing it thus perhaps preventing the hadronic phase from returning at high T [46]:

$$
\begin{aligned}
P_{\mathrm{QGP}} &= P_{\text{ideal QGP}} \\
&\quad -\alpha_S\left(\frac{11}{9}\pi T^4+\frac{2}{\pi}{\mu_q}^2T^2+\frac{{\mu_q}^4}{\pi^3}\right) \\
&\quad +\frac{8\alpha_S^{\frac{3}{2}}T}{3\pi^2\sqrt{2\pi}}\left(\frac{8\pi^2T^2}{3}+2\mu_q^2\right)^{\frac{3}{2}}
\end{aligned}
\tag{4.33}
$$

The coupling constant is a stongly varying function of the temperature T and sufficiently high orders have to be calculated so that the results are physically meaningful: at lower temperatures the coupling strength increases and high baryon densities it decreases so there is no region in the phase diagram where one may take a constant value of α_S. A model for α_S is required which extends from μ=0 to $\mu \sim 2$ GeV and furthermore spans the temperature range 0 MeV $\leq T \leq$ 200 MeV. The construction of such a model is clearly a formidable task.

Concluding then, our model for the phase transition is successful in the high-μ region but shows a severe deficiency at μ=0. This can perhaps be cured by including α_S corrections to the QGP pressure. A model for this important parameter is needed.

4.8 Alternative Proposal

In section 4.3 the concept of a shifted **quantum number chemical potential** was introduced. The basic idea was to include the volume of a hadron (V_0) in the thermodynamical description by modifying the chemical potential in a way so that the pressure retained its volume independent form. It is important to stress that the chemical potentials are conjugate to conserved charges i.e. quantum numbers and thus the problem of the returning hadronic phase at $\mu_B = 0$ was really to be expected (Figure 4.4).

In the following analysis, originally presented by [33], the chemical potentials are defined as usual in thermodynamics; they remain **particle chemical potentials.**

The analysis is based on Laplace transforming the excluded volume partition function. This enables one to prove that the pressure of a gas of extended particles is identical to that of a gas of pointlike particles provided that one modifies the chemical potentials.

Starting with a canonical partition function with a Van der Waals-like restriction on the volume $Z^{\mathrm{excl}}(T,N,V)$:

$$
Z^{\mathrm{excl}}(T,N,V) = Z(T,N,V-V_0N)\Theta(V-V_0N) \tag{4.34}
$$

where $\Theta(V - V_0N)$ is the usual step function. The grand canonical one follows from the above one as usual:

$$Z^{\text{excl}}(T,\mu,V) = \sum_{N=0}^{\infty} e^{(\frac{\mu N}{T})} Z(T,N,V - V_0N)\Theta(V - V_0N) \tag{4.35}$$

where the chemical potential μ is now conjugate to the particle number N. The dependence of the volume V on the particle number N prevents one to sum the series but this problem can be overcome by reverting to the pressure ensemble (isobaric partition function) as follows:

$$\begin{aligned} Z^{\text{excl}}(T,\mu,\xi) &= \int_0^{\infty} dV \, \exp(-\xi V) Z^{\text{excl}}(T,\mu,V) \\ &= \int_0^{\infty} dx \, \exp(-\xi x) Z(T,\overline{\mu},x) \end{aligned} \tag{4.36}$$

The last equation results from inserting equation (2) and then defining $\overline{\mu} = \mu - V_0T\xi$ and shifting the integration variable V to $x = V - V_0N$. The pressure can be proven to be [47]:

$$P^{\text{excl}}(T,\mu) = \lim_{V\to\infty} T\frac{\ln(Z^{\text{excl}}(T,\mu,V))}{V} = T\xi^*(T,\mu) \tag{4.37}$$

where ξ^* is the largest right singularity of the function $Z^{\text{excl}}(T,\mu,\xi)$ in the variable ξ. This has only one singular point, namely where the integral over x diverges at the upper limit; i.e. $x \to \infty$. Using the usual grand canonical definition of the pressure

$$P(T,\mu) = \lim_{V\to\infty} T\frac{\ln(Z(T,\mu,V))}{V} \tag{4.38}$$

for Z^{excl}, and using the fact that

$$\xi^* = \lim_{x\to\infty} \frac{\ln(Z(T,\overline{\mu},x))}{x} \tag{4.39}$$

with $\overline{\mu} = \mu - V_0T\xi^*$, gives the relationship between the extended and pointlike particle pressures:

$$P^{\text{excl}}(T,\mu) = P(T,\overline{\mu}) \;,\; \overline{\mu} = \mu - V_0P^{\text{excl}}(T,\mu). \tag{4.40}$$

The result for the pressure can most easily be obtained from the very definition of the grand canonical pressure partition function $\mathrm{Z}^{\text{pressure}}(T,\mu,P)$ [29]:

$$\begin{aligned} \mathrm{Z}^{\text{pressure}}(T,\mu,P) &= \int_0^{\infty} e^{-\frac{PV}{T}} Z(T,V,\mu)\, dV \\ &= \int_0^{\infty} e^{-\frac{V}{T}(P - \frac{T\ln Z}{V})}\, dV \end{aligned} \tag{4.41}$$

As a function of the pressure P, $\mathrm{Z}^{\mathrm{pressure}}(T,\mu,P)$ has a pole for

$$P = \frac{T \ln Z}{V}$$

The right hand side of the last equation is the pressure in the thermodynamical limit thus

$$P = \lim_{V\to\infty}\left(-\frac{\Omega}{V}\right) = \lim_{V\to\infty}\frac{T\ln Z}{V}$$

where Ω is the thermodynamic potential. Thus the pole of the isobaric partition function represents the pressure in the thermodynamic limit. Note that the result for the extended particle pressure is a recursive relation in $P^{\mathrm{excl}}(T,\mu)$. For clarity the densities of a few particle species are listed below (in the limit of Boltzmann statistics):

$$\begin{aligned}
n_{K+} &= \left[\int \frac{d^3p}{(2\pi)^3}\exp\left(-\frac{E}{T}+\frac{\mu_{K+}}{T}-\frac{P^{\mathrm{excl}}V_0}{T}\right)\right] \Big/ \left[1+V_0\sum_j n_j^{pt}\right] \\
n_{K-} &= \left[\int \frac{d^3p}{(2\pi)^3}\exp\left(-\frac{E}{T}+\frac{\mu_{K-}}{T}-\frac{P^{\mathrm{excl}}V_0}{T}\right)\right] \Big/ \left[1+V_0\sum_j n_j^{pt}\right] \\
n_{N} &= \left[\int \frac{d^3p}{(2\pi)^3}\exp\left(-\frac{E}{T}+\frac{\mu_{N}}{T}-\frac{P^{\mathrm{excl}}V_0}{T}\right)\right] \Big/ \left[1+V_0\sum_j n_j^{pt}\right] \\
n_{\overline{N}} &= \left[\int \frac{d^3p}{(2\pi)^3}\exp\left(-\frac{E}{T}+\frac{\mu_{\overline{N}}}{T}-\frac{P^{\mathrm{excl}}V_0}{T}\right)\right] \Big/ \left[1+V_0\sum_j n_j^{pt}\right]
\end{aligned} \tag{4.42}$$

where the sum $\sum_j n_j^{pt}$ runs over <u>all</u> pointlike particle densities in the gas.

It is clear that **particle chemical potentials** are being used, these are related to the **quantum chemical potentials** by the following relations (the subscript N refers to the nucleon):

$$\begin{aligned}
\overline{\mu_B} &= \frac{\overline{\mu_N} - \overline{\mu_{\overline{N}}}}{2} \\
&= \frac{\mu_N - \mu_{\overline{N}}}{2} \\
&= \mu_B
\end{aligned} \tag{4.43}$$

Thus the baryon chemical potential μ_B does not change when one introduces the hard-core repulsion. For $n_B = 0$ one has $\mu_B = 0 = \overline{\mu_B}$, there is thus no contradiction with the Gibb's equilibrium conditions. However, the chemical potentials of the particles and antiparticles are the same at this point because of the pressure term.

Expressions for the excluded particle density, entropy density and energy density are given in the reference under equations (11), (12) and (13). What I wish to point out here is this formulation does not have the problem of the returning hadronic phase at $\mu_B = 0$. This is because the quantum number correction factor

$$(1 + V_0 n_B^0)^{-1} \text{ or } (1 + V_0(n_B^0 + n_S^0))^{-1}$$

gives the pointlike particle density at $\mu_B = 0$ whereas in the present formulation the excluded volume particle density n_i^{excl} is replaced by a sum over all particles j whose (particle) chemical potential is not zero. The proof is as follows (here pt refers to pointlike quantities):

$$\begin{aligned} n_i^{\text{excl}} &= \frac{\partial P^{\text{excl}}}{\partial \mu_{pt}^i} \\ &= \sum_j \frac{\partial P^{\text{excl}}}{\partial \overline{\mu_j}} \frac{\partial \overline{\mu_j}}{\partial \mu_{pt}^i} \\ &= \sum_j n_j^{pt} \left[\delta_{ij} - V_0 n_i^{\text{excl}}\right] \\ &= n_i^{pt} - V_0 n_i^{\text{excl}} \sum_j n_j^{pt} \end{aligned} \tag{4.44}$$

thus

$$n_i^{\text{excl}} = \frac{n_i^{pt}}{1 + V_0 \sum_j n_j^{pt}} \tag{4.45}$$

This concludes the proof.

For the excluded baryon density n_B^{excl} the equation reads

$$n_B^{\text{excl}} = \frac{n_B^{pt}}{1 + V_0 \sum_j n_j^{pt}} \tag{4.46}$$

Note that the above correction factor implies that particle interactions are not selective; although the proton-antiproton cross-section is much larger than the proton-proton one, the correction factor implies that the reactions occur at the same strength. This is because one corrects proportional to the total -and not the net- particle density in the gas.

4.9 Conclusion

It is clear that the point-like particle formulation of the phase transition of nuclear matter to the quark gluon plasma is insufficient because the volume of the hadrons defines the dense

packing limit which is an essential ingredient of the process. This feature has been included in a thermodynamically consistent description of modified quantum number chemical potentials. With these the phase diagrams have been calculated for the case where only the baryon chemical potential has been shifted and for the case where both (baryon and strange chemical potential) have been modified. The difference between the two formulations becomes apparent in the high baryon density region where the asymmetric shift shows kaon condensation while the symmetric change does not. The baryon density (defined by μ_B^0) at the phase transition is the same in both formulations.

Volume corrections that are proportional to conserved quantities which vanish at $\mu_B = 0$ allow the hadronic phase to reappear at high T. This unphysical feature could be avoided by including strong coupling constant corrections to the quark gluon plasma which have been shown to add to the pressure of it, thus perhaps preventing the hadronic phase from reappearing. However, this is a rather ad-hoc cure to the formulation which is not neccessary in that of [33] where the correction factors are proportional to the total particle number density. Although this formulation is rather difficult to implement and is of a geometric type thus assuming that all particles interact with each other with equal strength, it does not have the problem of the quantum number formulation at high T and $\mu_B = 0$.

Acknowledgements

I would like to thank my supervisor, Prof. J. Cleymans, for his advice and support during this work and throughout my career. Also, I am indebted to Prof. E. Suhonen for the ideas on the modified chemical potentials.

Without the help of the secretaries in Bielefeld and Cape Town this work and the transition Cape Town-Bielefeld would not have gone so smoothly as it has; a special thanks to Mrs J. Parsons and Frau G. Eickmeyer.

Other people who helped me significantly in Cape Town were: M. Murray (computers), K. Henry (moral support and all the rest) and my family and friends.

Appendix A

Analytic Results

In this Appendix some of the important analytic results that have been used in the previous chapters will be listed. In order expressions for

- the density of an ideal, relativistic, massless fermion gas
- the pressure of an ideal, relativistic,massless fermion gas
- the pressure of an ideal, relativistic gluon gas
- the density of an ideal, relativistic, low temperature fermion gas
- the pressure of an ideal, relativistic, low temperature fermion gas

will be developed.

Density of massless fermion gas

In a relativistic fermion gas the conserved quantity is the charge Q conjugate to its chemical potential μ. In the Grand Canonical formalism the expressions for the charge densities are (for degeneracy g_i):

$$n = \frac{g_i}{2\pi^2}\int_0^\infty \frac{p^2\,dp}{\exp(\frac{E-\mu}{T})+1} \tag{A.1}$$

$$\overline{n} = \frac{g_i}{2\pi^2}\int_0^\infty \frac{p^2\,dp}{\exp(\frac{E+\mu}{T})+1} \tag{A.2}$$

with $E = p$ in the zero mass approximation. Defining $x = \frac{p-\mu}{T}$ one splits integral (1) into a finite and an infinite term:

$$n = \frac{g_i T^3}{2\pi^2}\left[\int_{-\frac{\mu}{T}}^0 \frac{(x+\frac{\mu}{T})^2\,dx}{\exp(x)+1} + \int_0^\infty \frac{(x+\frac{\mu}{T})^2\,dx}{\exp(x)+1}\right] \tag{A.3}$$

For the antiparticles the substitution is $x = \frac{p+\mu}{T}$ and thus

$$\overline{n} = \frac{g_i T^3}{2\pi^2}\left[-\int_0^{\frac{\mu}{T}} \frac{(x-\frac{\mu}{T})^2\,dx}{\exp(x)+1} + \int_0^{\infty} \frac{(x-\frac{\mu}{T})^2\,dx}{\exp(x)+1}\right] \tag{A.4}$$

Letting x → −x in the last (finite) integral and using the identity

$$\frac{1}{\exp(-x)+1} = 1 - \frac{1}{\exp(x)+1} \tag{A.5}$$

one obtains for the conserved charge density Q: (the first term in equation (3) is cancelled)

$$Q = n - \overline{n} = \frac{g_i T^3}{2\pi^2}\left[\int_{\frac{-\mu}{T}}^{0} (x+\frac{\mu}{T})^2\,dx + \int_0^{\infty} \frac{4x\frac{\mu}{T}\,dx}{\exp(x)+1}\right] \tag{A.6}$$

These integrals are elementary and are solved to be:

$$n - \overline{n} = g_i(\frac{\mu T^2}{6} + \frac{\mu^3}{6\pi^2}) \tag{A.7}$$

A.1 Pressure of massless fermion gas

The pressure of a massless fermion gas reads

$$P = \frac{g_i}{6\pi^2}\left[\int_0^{\infty} \frac{p^3\,dp}{\exp(\frac{p-\mu}{T})+1} + \int_0^{\infty} \frac{p^3\,dp}{\exp(\frac{p+\mu}{T})+1}\right] \tag{A.8}$$

Using the same substitutions as before one finds that the pressure P reads:

$$P = g_i\left(\frac{7\pi^2 T^4}{360} + \frac{T^2\mu^2}{12} + \frac{\mu^4}{24\pi^2}\right) \tag{A.9}$$

Since the expression for the energy density ϵ differs only by a factor 3 it is clear that

$$P = \frac{1}{3}\epsilon\,. \tag{A.10}$$

A.2 Pressure of a gluon gas

Since the number of gluons is not a conserved quantity one does not associated a chemical potential for them (the analogy is the photon in the Abelian U(1) theory Quantum Electrodynamics) and so the pressure P is simply:

$$\begin{aligned} P &= \frac{g_i}{2\pi^2}\int_0^{\infty} \frac{p^3\,dp}{\exp(\frac{p}{T})-1} \\ &= \frac{g_i T^4 \pi^4}{6\pi^2 15} \\ &= \frac{8\pi^2 T^4}{45} \end{aligned} \tag{A.11}$$

The degeneracy of the gluon gas is 8 colours and 2 polarisations.

A.3 The density of a low T fermion gas

Unlike bosons and antifermions the low temperature behaviour of a fermion gas is not Boltzmannian if $\mu > m$; it is dictated by the Fermi-Dirac box-like distribution present at zero T. The following development is vaild for $\mu > m$; i.e. the fermions are generated by the chemical potential and not by thermal production as is the case when $\mu < m$ where the distribution is Boltzmannian.

The density integral reads:

$$n = \frac{g_i}{2\pi^2}\int_0^\infty \frac{p^2\,dp}{\exp(\frac{E-\mu}{T})+1} \tag{A.12}$$

and is converted to an integral over energy using $p\,dp = E\,dE$:

$$n = \frac{g_i}{2\pi^2}\int_m^\infty \frac{\sqrt{(E^2-m^2)}E\,dE}{\exp(\frac{E-\mu}{T})+1} \tag{A.13}$$

The substitution $x = \frac{E-\mu}{T}$ allows one to rewrite the integral as:

$$n = \frac{g_i T^3}{2\pi^2}\int_{\frac{m-\mu}{T}}^\infty \frac{(x+(\frac{\mu}{T}))\sqrt{(((x+(\frac{\mu}{T}))^2-(\frac{m}{T})^2)}\,dx}{\exp(x)+1} \tag{A.14}$$

Splitting the integral into a finite and an infinite piece and making the transformation $x \to -x$ on the finite piece, then making use of the identity

$$\frac{1}{\exp(-x)+1} = 1 - \frac{1}{\exp(x)+1} \tag{A.15}$$

leaves one with the following result:

$$\begin{aligned} n = \frac{g_i T^3}{2\pi^2} \quad & \left[\int_0^\infty \frac{(x+(\frac{\mu}{T}))\sqrt{((x+(\frac{\mu}{T}))^2-(\frac{m}{T})^2)}\,dx}{\exp(x)+1}\right. \\ & + \int_0^{\frac{\mu-m}{T}} ((\frac{\mu}{T})-x)\sqrt{((\frac{\mu}{T})-x)^2-(\frac{m}{T})^2}\,dx \\ & \left. + \int_0^{\frac{\mu-m}{T}} \frac{(x-(\frac{\mu}{T}))\sqrt{(((\frac{\mu}{T})-x)^2-(\frac{m}{T})^2)}\,dx}{\exp(x)+1}\right] \end{aligned} \tag{A.16}$$

In the limiting case where $\frac{\mu-m}{T} \to \infty$ the above integrals reduce to a zero T contribution and a finite T term:

$$\begin{aligned} n = \quad & \frac{g_i}{2\pi^2}\left[\frac{1}{3}(\mu^2-m^2)^{\frac{3}{2}}\right. \\ & \left. + T^3\int_0^\infty \frac{(x+\frac{\mu}{T})\sqrt{((x+(\frac{\mu}{T}))^2-(\frac{m}{T})^2)}-(\frac{\mu}{T}-x)\sqrt{(((\frac{\mu}{T})-x)^2-(\frac{m}{T})^2)}\,dx}{\exp(x)+1}\right. \end{aligned} \tag{A.17}$$

The procedure now is to expand the numerator in a Taylor series in powers of x. The exponential damping in the denominator justifies this approximation.
Since the function one is expanding is of the form

$$\int_0^\infty \frac{dx}{\exp(x)+1}\Big(f(x)-f(-x)\Big) \tag{A.18}$$

only odd powers remain when expanding $f(x)-f(-x)$. The $\mathcal{O}(1)$ term is:

$$n_{\mathcal{O}(1)} = \frac{g_i}{2\pi^2}\frac{\pi^2T^2}{6}\left[\frac{\mu^2}{\sqrt{\mu^2-m^2}}+\sqrt{\mu^2-m^2}\right] \tag{A.19}$$

The $\mathcal{O}(3)$ term is:

$$n_{\mathcal{O}(3)} = \frac{7\pi^4T^4}{120}\left[\frac{1}{\sqrt{\mu^2-m^2}}+\frac{\mu^4}{(\mu^2-m^2)^{\frac{5}{2}}}-\frac{2\mu^2}{(\mu^2-m^2)^{\frac{3}{2}}}\right] \tag{A.20}$$

Collecting the terms one finds the low temperature fermion density corresponding to the chemical potential μ to be

$$\begin{aligned} n = \frac{g_i}{2\pi^2}\Bigg[&\frac{(\mu^2-m^2)^{\frac{3}{2}}}{3}+\frac{\pi^2T^2}{6}\left(\frac{\mu^2}{\sqrt{\mu^2-m^2}}+\sqrt{\mu^2-m^2}\right)\\ &+\frac{7\pi^4T^4}{120}\left(\frac{1}{\sqrt{\mu^2-m^2}}+\frac{\mu^4}{(\mu^2-m^2)^{\frac{5}{2}}}-\frac{2\mu^2}{(\mu^2-m^2)^{\frac{3}{2}}}\right)\Bigg]\\ &+\mathcal{O}(T^6) \end{aligned} \tag{A.21}$$

A.4 The pressure of a low T fermion gas

The standard integral for the infinite volume expression for the pressure is

$$P = \frac{g_i}{2\pi^2}\int_0^\infty \frac{p^4\,dp}{3E\left(\exp\left(\frac{E-\mu}{T}\right)+1\right)} \tag{A.22}$$

which is converted to an integral over energy to give:

$$P = \frac{g_i}{6\pi^2}\int_m^\infty \frac{(E^2-m^2)^{\frac{3}{2}}\,dE}{\exp\left(\frac{E-\mu}{T}\right)+1} \tag{A.23}$$

With the substitution $x = \frac{E-\mu}{T}$ and making use of equation (15) after changing $x \to -x$ in the finite part of the integral one obtains an identity for the pressure in terms of finite and infinite integrals of the following form:

$$P = \frac{g_i T^4}{6\pi^2} \left[\int_0^{\frac{\mu-m}{T}} ((\frac{\mu}{T} - x)^2 - (\frac{m}{T})^2)^{\frac{3}{2}}\, dx + \int_0^{\infty} \frac{((x+\frac{\mu}{T})^2 - (\frac{m}{T})^2)^{\frac{3}{2}}\, dx}{\exp(x)+1} - \int_0^{\frac{\mu-m}{T}} \frac{((\frac{\mu}{T} - x)^2 - (\frac{m}{T})^2)^{\frac{3}{2}}\, dx}{\exp(x)+1} \right] \tag{A.24}$$

The first term is the zero T contribution to the pressure and may be integrated to give

$$P_{T=0} = \frac{g_i}{6\pi^2}\left(\frac{\mu(\mu^2-m^2)^{\frac{3}{2}}}{4} - \frac{3m^2\mu\sqrt{(\mu^2-m^2)}}{8} + \frac{3m^4}{8}\ln(\frac{\mu+\sqrt{\mu^2-m^2}}{m}) \right) \tag{A.25}$$

The remainder of the terms are dealt with as previously; under the strict assumption that $\frac{\mu-m}{T} \to \infty$ one obtains the first order correction to the pressure (in the variable x):

$$P_{\mathcal{O}(1)} = \frac{g_i}{6\pi^2}\frac{\pi^2 T^2}{2}\mu\sqrt{(\mu^2-m^2)} \tag{A.26}$$

and a third order correction of

$$P_{\mathcal{O}(3)} = \frac{g_i}{6\pi^2}\frac{7\pi^4 T^4}{120}\left(\frac{3\mu}{\sqrt{(\mu^2-m^2)}} - \frac{\mu^3}{(\mu^2-m^2)^{\frac{3}{2}}} \right) \tag{A.27}$$

Collecting all the terms one finds a pressure P given by

$$P = \frac{g_i}{6\pi^2} \left[\frac{\mu(\mu^2-m^2)^{\frac{3}{2}}}{4} - \frac{3m^2\mu\sqrt{(\mu^2-m^2)}}{8} + \frac{3m^4}{8}\ln\left(\frac{\mu+\sqrt{\mu^2-m^2}}{m}\right) + \frac{\pi^2 T^2}{2}\mu\sqrt{(\mu^2-m^2)} + \frac{7\pi^4 T^4}{120}\left(\frac{3\mu}{\sqrt{(\mu^2-m^2)}} - \frac{\mu^3}{(\mu^2-m^2)^{\frac{3}{2}}} \right) \right] + \mathcal{O}(T^6) \tag{A.28}$$

Bibliography

[1] K. Redlich and L.Turko, Z. Phys. **C5** (1980) 201 and L. Turko, Phys. Lett **104B** (1981) 153.

[2] J. Kapusta, Finite Temperature Field Theory, Cambridge University Press (1989)

[3] H.-TH. Elze, W. Greiner and J. Rafelski, Phys. Lett. **B124** (1983) 515.

[4] R. Hagedorn and K. Redlich, Z. Phys. **C27** (1985) 541.

[5] P. Koch, Diploma Thesis, University Frankfurt, 1983 (unpublished)

[6] J. Cleymans, E. Suhonen and G.M Weber, Z. Phys. **C53** (1992) 485.

[7] C. Derreth, W. Greiner, H.-Th. Elze and J. Rafelski, Phys. Rev. **C31** (1985) 1360.

[8] A. Capella, Orsay preprint LPTHE 91/37.

[9] O. Villallobos Baillie, Nucl. Phys. **A525** (1991) 189c.

[10] J. Schuhkraft, Cern preprint PPE 91-04.

[11] J. Cleymans, H. Satz, E. Suhonen and D.W. von Oertzen, Phys. Lett. **242B** (1990) 111.

[12] J. Cleymans, K. Redlich and E. Suhonen, Z. Phys. **C51** (1991) 137.

[13] N.J. Davidson, H.G. Miller, R.M. Quick and J. Cleymans, Phys. Lett. **B255** (1991) 105 and N.J. Davidson, H.G. Miller and D.W. von Oertzen Phys. Lett. **B256** (1991) 554.

[14] U. Heinz and K.S. Lee, Phys. Lett. **B259** (1991) 162.

[15] J.D. Bjorken, Phys. Rev. **D27** (1983) 140.

[16] British Scandinavian Collab., B. Alper et al. Nucl Phys. **B100** (1975) 237.

[17] E802 Collaboration: T. Abbott et al., Phys. Rev. Lett. **64** (1990) 847.

[18] WA85 Collaboration: S. Abatzis et al., Phys. Lett. **B244** (1990) 130; Phys. Lett. **B259** (1991) 508.

[19] NA35 Collaboration: J. Bartke et al., Z. Phys. **C48** (1990) 191.

[20] E. Suhonen, J. Cleymans and J. Stålnacke, Nuclear Physics B (Proc. Suppl.) **24B** (1991) 260.

[21] R. Hagedorn, CERN yellow report 71-12 (1971).

[22] J. Sollfrank, P. Koch and U. Heinz, Z. Phys. **C52** (1991) 593.

[23] S. Gavin and P.V. Ruuskanen, Phys. Lett. **B262** (1991) 326.

[24] B. Lukács, J. Zimányi and N.L. Balazs, Phys. Lett. **B183** (1987) 27.

[25] K.S. Lee, M.J. Rhoades-Brown and U. Heinz, Phys. Lett. **B174** (1986) 123.

[26] J. Cleymans, K. Redlich, H. Satz and E. Suhonen, Z. Phys. **C33** (1986) 151.

[27] V.V. Dixit and E. Suhonen, Z. Phys. **C18** (1983) 355.

[28] J. Cleymans and E. Suhonen, Z. Phys. **C37** (1987) 51.

[29] A.G. Schnabel, Preprint UCT-TP 97/88. Cape Town, 1988 (unpublished).

[30] K. Olive, Nucl. Phys. **B198** (1982) 461 and Nucl. Phys. **B190** (1981) 483.

[31] D. Anchishkin, K.A. Bugaev, M.I. Gorenstein and E. Suhonen, Z. Phys. **C45** (1990) 687.

[32] R. Hagedorn, Z. Phys. **C17** (1983) 265.

[33] D.H. Rischke, M.I Gorenstein, H. Stöcker and W. Greiner, Z. Phys. **C51** (1991) 485.

[34] J. Cleymans, J. Stålnacke, E. Suhonen and G.M. Weber, Z. Phys. C (to appear).

[35] H.W. Barz, B.L. Friman, J. Knoll and H. Schulz, Phys. Rev **D40** (1989) 157.

[36] J. Cleymans and D.W. von Oertzen, Phys. Lett. **B249** (1990) 511.

[37] H. Kouno and F. Takagi, Z. Phys. **C42** (1989) and Z. Phys. **C45** (1989) 209.

[38] R.K. Pathria: Statistical Mechanics, Pergamon Press (1972)

[39] H.E Haber and H.A. Weldon, Phys. Rev. Lett. **46** (1981) 1497.

[40] K.M. Benson, J. Bernstein and S. Dodelson, Phys. Rev. **D44** (1991) 2480.

[41] D.B. Kaplan and A.E. Nelson, Phys. Lett. **B175** (1986) 57.

[42] A.E. Nelson and D.B. Kaplan, Phys. Lett. **B192** (1987) 193.

[43] N.J. Davidson and H.G. Miller, Phys. Lett. **B255** (1991) 110.

[44] J. Cleymans and E. Suhonen, "Hadron Structure '91", Proceedings of the Meeting in Stará Lesná, (1991) Ed. L. Martinovič pp. 106-118.

[45] B. Müller: The Physics of the Quark Gluon Plasma, Springer (1985).

[46] S. Uddin and C. P. Singh, Z. Phys. **C53** (1992) 319.

[47] M.I. Gorenstein, V.K. Petrov and G.M. Zinovjev, Phys. Lett. **B106** (1981) 327.